

Continuous estimation of anthropogenic CO₂: Model-based evaluation of CO₂, CO, δ¹³C(CO₂) and Δ¹⁴C(CO₂) tracer methods

S.N. Vardag¹, C. Gerbig², G. Janssens-Maenhout³, I. Levin¹

[1]{Institut für Umweltphysik, Heidelberg University, Germany}

[2]{Max Planck Institute for Biogeochemistry, Hans-Knöll-Str.10, 07745 Jena, Germany}

[3]{European Commission, Joint Research Centre, Ispra, Via Fermi, 2749, 21027 Ispra, Italy}

Correspondence to: S.N. Vardag (svardag@iup.uni-heidelberg.de)

Abstract

We investigate different methods for estimating anthropogenic CO₂ using modelled continuous atmospheric concentrations of CO₂ alone, as well as CO₂ in combination with the surrogate tracers CO, δ¹³C(CO₂) and Δ¹⁴C(CO₂). These methods are applied at three hypothetical stations representing rural, urban and polluted conditions. We find that independent of the tracer used, an observation-based estimate of continuous anthropogenic CO₂ is not yet feasible at rural measurement sites due to the low signal to noise ratio of anthropogenic CO₂ estimates at such settings. The tracers δ¹³C(CO₂) and CO provide an accurate possibility to determine anthropogenic CO₂ continuously, only if all CO₂ sources in the catchment area are well characterized or calibrated with respect to their isotopic signature and CO to anthropogenic CO₂ ratio. We test different calibration strategies for the mean isotopic signature and CO to CO₂ ratio using precise Δ¹⁴C(CO₂) measurements on monthly-integrated as well as on grab samples. For δ¹³C(CO₂), a calibration with annually averaged ¹⁴C(CO₂) grab samples is most promising, since integrated sampling introduces large biases into anthropogenic CO₂ estimates. For CO, these biases are smaller. The precision of continuous anthropogenic CO₂ determination using δ¹³C(CO₂) depends on measurement precision of δ¹³C(CO₂) and CO₂ while the CO-method is mainly limited by the variation of natural CO sources and sinks. At present, continuous anthropogenic CO₂ could be determined using the tracers δ¹³C(CO₂) and/or CO with a precision of about 30%, a mean bias of about 10% and without significant diurnal discrepancies. Hypothetical future measurements of continuous Δ¹⁴C(CO₂) with a precision of 5 ‰ are promising for anthropogenic CO₂ determination (precision ca. 10-20%) but they are not available yet. The investigated tracer-based approaches open the door to improving,

1 validating and reducing biases of highly resolved emission inventories using atmospheric
2 observation and regional modelling.

3

4 **1. Introduction**

5 Earth's carbon budget is strongly influenced by anthropogenic CO₂ emissions into the atmosphere
6 (Keeling et al., 1996, Le Quéré et al., 2015). In order to support studies of the carbon cycle and to
7 determine net and gross carbon fluxes quantitatively, various measurement sites monitor the
8 atmospheric CO₂ mole fraction worldwide. In top-down approaches and in conjunction with
9 atmospheric transport models, these CO₂ measurements are used to infer total CO₂ emissions
10 (Bousquet et al., 2000; Gurney et al., 2002; Peylin et al., 2013), but a differentiation into biogenic,
11 oceanic and anthropogenic CO₂ sources and sinks is not feasible with CO₂ concentration
12 measurements alone. Inverse model studies commonly utilize anthropogenic CO₂ emission
13 inventories to estimate anthropogenic CO₂ and are then able to separate anthropogenic from
14 biogenic or oceanic carbon sink and source influences. However, currently available emission
15 inventories exhibit large discrepancies between each other of about 10-40% at the country level
16 (Peylin et al., 2011), and increase further with decreasing spatial scale (Gurney et al., 2005). These
17 discrepancies suggest that biases may be in the order of about 70-100 % for highly resolved
18 (0.1°x0.1°) data sets and uncertainties (1σ) of emission inventories may be between 30-150 %
19 (Wang et al., 2013). In order to better study and quantify the biospheric carbon fluxes, their
20 underlying processes and potential feedbacks, it is desirable to reduce the current uncertainties as
21 well as biases of emission inventories. Validation and improvement of emission inventories
22 requires accurate and precise anthropogenic CO₂ estimates (as well as accurate and precise
23 transport models) on all relevant time scales ranging from hours to years. We hereafter refer to
24 anthropogenic CO₂ as fuel CO₂ and include non-combustion emissions such as emissions from
25 cement industry or non-energy use of fuels as well as agricultural waste burning. Fossil fuel CO₂
26 excludes all contributions from biofuel emissions or from agricultural waste burning. We define
27 biofuel CO₂ as non-fossil fuel CO₂ released during combustion, including solid (e.g. wood, waste,
28 charcoal, municipal renewable waste, bagasse, vegetal waste and dung), liquid (e.g. biodiesel, bio
29 gasoline and black liquor) and gaseous (from compost or cattle farm) biomaterial. It does not
30 include large-scale biomass burning. For some purposes e.g., when validating fossil fuel emission
31 reductions, it may actually be advantageous to estimate only the fossil fuel CO₂ contribution, which

1 is the fuel CO₂ contribution without biofuel CO₂. However, when solving for biospheric fluxes, the
2 biofuel CO₂ is important as well, since it equally contributes to the instantaneously measured CO₂
3 concentration and needs to be separated from the biospheric flux. In the following, we seek to
4 constrain the fuel CO₂ (fossil fuel CO₂ plus biofuel CO₂).

5
6 ¹⁴C measurements are commonly used as surrogate to differentiate between biogenic and fossil fuel
7 CO₂ contributions in the atmosphere, since fossil fuels do not contain any ¹⁴C, in contrary to
8 biogenic sources (Levin et al., 2003). The ¹⁴C/C isotope ratio in CO₂ is expressed on the Δ¹⁴C(CO₂)
9 scale, which denotes the deviation of the ¹⁴C/C ratio in CO₂ from a standard material in permil
10 (Stuiver and Polach, 1977). We use the depletion of Δ¹⁴C(CO₂) at a polluted measurement site
11 relative to Δ¹⁴C(CO₂) in clean background air to derive quantitative information on the contribution
12 of fossil fuel CO₂ to total measured CO₂ mole fraction at the polluted site. Radiocarbon (¹⁴C) is
13 thus used as quantitative tracer for fossil fuel contributions (e.g. Levin et al., 2003; Levin and
14 Karstens, 2007; Turnbull et al., 2006; Turnbull et al., 2015; Newman et al., 2015). However, there
15 are a number of problems, when using ¹⁴C(CO₂) as tracer for anthropogenic emissions: First,
16 precise Δ¹⁴C(CO₂) measurements from conventional counting or accelerator mass spectrometry
17 (AMS) (better than 2 ‰) are time and cost intensive, thus currently prohibiting the coverage of
18 large periods and large area of such measurements. Attempts have been made to sample ¹⁴C(CO₂)
19 with a higher measurement frequency using gas chromatography (GC) coupled to continuous-flow
20 AMS (McIntyre et al., 2013), but the technique is not applicable to atmospheric ¹⁴C samples so far
21 and the precision in Δ¹⁴C(CO₂) is lower than for AMS or conventional counting. This results in
22 less precise fossil fuel CO₂ estimates. These studies indicate, however, that the measurement
23 precision using GC and continuous-flow AMS may reach 5 ‰ in future. The benefit of such
24 hypothetical quasi-continuous but reduced precision fossil fuel CO₂ estimates is assessed for the
25 first time in this work in order to check if these measurements would provide beneficial constraints
26 for determining CO₂ continuously.

27 Second, a complication of applying Δ¹⁴C(CO₂) measurements for fossil fuel CO₂ estimation is that
28 nuclear power plants as well as nuclear fuel reprocessing plants emit ¹⁴C(CO₂) and can bias regional
29 Δ¹⁴C(CO₂)-based estimates of fossil fuel contributions if not taken into account (Levin et al., 2003;
30 Graven and Gruber, 2011, Vogel et al., 2013b). Moreover, biofuel CO₂ contributions cannot be
31 monitored with Δ¹⁴C(CO₂) measurements, since they have a similar Δ¹⁴C(CO₂) signature as the

1 biosphere or may even be elevated in ^{14}C due to the bomb radiocarbon $^{14}\text{C}(\text{CO}_2)$ stored in wood
2 material. This could become especially problematic, since the use of biofuels is expected to play
3 an increasingly important role for the energy supply in the near future (Coyle, 2007). Recognizing
4 these shortcomings of $\Delta^{14}\text{C}(\text{CO}_2)$ as tracer for anthropogenic CO_2 , it is worth considering other
5 tracers for the estimation of fuel CO_2 contributions.

6
7 Turnbull et al. (2015) have shown that for an urban study area in the middle of the North American
8 continent, the local CO_2 offset relative to clean air, ΔCO_2 , can be used as tracer for fuel CO_2
9 contributions, if all other CO_2 sources and sinks, such as from the living biosphere, are negligible.
10 This may be the case for wintertime periods in urban areas when using a background station upwind
11 and close to the urban area. However, we do not expect ΔCO_2 to be a quantitative tracer when
12 biospheric fluxes occur within the study area. This is normally the case in spring, summer and
13 autumn.

14 Since CO is often co-emitted during (incomplete) combustion and since CO can be measured
15 continuously, the CO offset relative to clean air, ΔCO , is frequently used as tracer for fuel CO_2
16 (Meijer et al., 1996; Gamnitzer et al., 2006; Rivier et al., 2006; Turnbull et al., 2006; Levin and
17 Karstens, 2007; Vogel et al., 2010, Turnbull et al., 2011; Newman et al., 2013). If the mean ratio
18 of the CO offset (Δx) relative to the fuel CO_2 offset (Δy_{F}), i.e. $\Delta x/\Delta y_{\text{F}} \equiv \overline{R_{\text{F}}}$, is known and relatively
19 constant within one month, it is principally possible to derive a continuous Δy_{F} estimate from Δx
20 measurements by dividing Δx by monthly mean $\overline{R_{\text{F}}}$. The overbar shall emphasize that we use one
21 averaged value for R_{F} , even though it actually varies with the relative fraction of the different
22 emission groups in a varying catchment area of the measurement site. CO is also produced during
23 oxidation of methane and hydrocarbons, particularly during summer (Granier et al., 2000). The
24 main sinks of CO are photo-oxidation and reaction with OH (Parrish et al., 1993) as well as soil
25 uptake (Inman et al., 1971), leading to a rather short atmospheric lifetime of CO of several weeks
26 in summer (Prather et al., 2011). Natural CO sinks and sources vary on time scales of hours to
27 seasons. Further, relative contributions of different fuel CO_2 sectors (e.g. energy production, road
28 traffic, residential heating, industrial emissions etc.) with different emission ratios ($\Delta\text{CO}/\Delta\text{CO}_2$),
29 may vary on short time scales of hours to longer time scales of years, if e.g. combustion
30 technologies, processes and procedures change in the long-term. Therefore, the mean $\overline{R_{\text{F}}} (= \Delta x/\Delta y_{\text{F}})$
31 is a function of space and time and might need to be calibrated using e.g. $\Delta^{14}\text{C}(\text{CO}_2)$ measurements

1 (Levin and Karstens, 2007). If $\overline{R_F}$ does not vary significantly within the time scale of the
2 calibration, continuous Δ_{yF} can be estimated. However, if $\overline{R_F}$ varies strongly on time scales of
3 smaller than the calibration interval, further corrections (e.g. diurnal or seasonal) may be necessary
4 (Vogel et al., 2010). These corrections are only reliable if $\overline{R_F}$ variations are systematic. Since this
5 is not always the case, additional or other continuous tracers may need to be considered to improve
6 fuel CO₂ estimates.

7 One of these tracers may be $\delta^{13}\text{C}(\text{CO}_2)$, since fuel emissions tend to be more depleted in ¹³CO₂
8 than fluxes from the biosphere. Zondervan and Meijer (1996), Pataki et al. (2006) and Djuricin et
9 al. (2010) have attempted to estimate fuel CO₂ emissions in specific case studies using mass
10 spectrometric measurements of $\delta^{13}\text{C}(\text{CO}_2)$, in addition to $\Delta^{14}\text{C}(\text{CO}_2)$ measurements. Recently, new
11 optical instrumentation allows measuring $\delta^{13}\text{C}(\text{CO}_2)$ continuously (e.g. Esler et al., 2000; Tuzson
12 et al., 2011; Hammer et al., 2013; Vogel et al., 2013a) and thus open the door for $\delta^{13}\text{C}(\text{CO}_2)$ as a
13 continuous tracer for fuel CO₂ contributions. In order to use $\delta^{13}\text{C}(\text{CO}_2)$ measurements at an urban
14 site, the mean isotopic signature of the sources (and sinks) in the catchment area of the site, $\overline{\delta_F}$,
15 must be known and relatively constant (Newman et al., 2015) and potentially require calibration
16 (as discussed for CO). Further, the signature of fuel CO₂ emissions must be significantly different
17 from biospheric CO₂ emissions in order to differentiate properly between them.

18 In many settings, we will exhibit neither a constant ratio $\overline{R_F}$ nor a constant fuel source signature
19 $\overline{\delta_F}$. This will especially be the case if multiple sources (i) with different emission ratios $\overline{R_{F,i}}$ and
20 different fuel $\delta^{13}\text{C}(\text{CO}_2)$ source signatures $\delta_{F,i}$ are located in the catchment area of the measurement
21 site. In these cases, it may be advantageous to divide the fuel emissions into (two) different groups.
22 CO will only be an adequate tracer for a certain emission group, if this group has a significantly
23 different ratio $\overline{R_F}$ ($=\Delta x/\Delta y_F$) than any other emission group. In analogy, $\delta^{13}\text{C}(\text{CO}_2)$ will only be a
24 good tracer for a certain emission group if the group's emissions are significantly more depleted
25 or enriched with respect to the other groups. If we divide all fuel CO₂ contributions into two
26 emission groups, of which one is well constrained by CO and the other by $\delta^{13}\text{C}(\text{CO}_2)$, we may then
27 join both tracers to determine the total fuel CO₂ contributions. In several published studies, the CO
28 mole fraction has been used as a tracer for traffic emissions only (e.g. Schmidt et al., 2014), since
29 these often exhibit high $\Delta\text{CO}/\Delta\text{CO}_2$ ratios. However, in some regions, emission inventories (e.g.
30 Landesamt für Umwelt, Messungen und Naturschutz Baden-Württemberg, available at:

1 <http://www.ekat.baden-wuerttemberg.de/>) depict that the emission ratio \overline{R}_{tr} ($=\Delta x/\Delta y_{tr}$) has been
2 decreasing during the last decade, degrading CO as a tracer for traffic contributions. At the same
3 time, diesel/petrol for vehicle is blended with an increasing amount of biodiesel/bio gasoline (for
4 OECD countries to the order of 5 %, (IEA, 2014)). More in general, emission inventories show
5 that (the sum of solid, liquid and gaseous) biofuel CO₂ emissions in OECD countries have increased
6 (IEA, 2014) and that the mean emission ratio of biofuel emissions \overline{R}_{bf} ($=\Delta x/\Delta y_{bf}$) is very high
7 (EDGARv4.3 emission inventory (EC-JRC/PBL, 2015)), qualifying CO as a tracer for biofuel
8 contributions. However, the emission ratio varies depending on the combustion type. Later we
9 examine separately, if these two emission groups, traffic and biofuel emissions, could possibly be
10 traced with CO.

11 In the present study, we investigate how continuous CO₂, CO, $\delta^{13}\text{C}(\text{CO}_2)$ and $\Delta^{14}\text{C}(\text{CO}_2)$
12 measurements as well as the combination of these tracers could be used to estimate continuous fuel
13 CO₂. In order to validate how precisely and accurately we may be able to determine fuel CO₂ using
14 continuous (hourly) CO₂, CO, $\delta^{13}\text{C}(\text{CO}_2)$ and $\Delta^{14}\text{C}(\text{CO}_2)$ as tracers, we use a modelled data set, in
15 which, contrary to measured data sets, CO₂ contributions from all source categories, i.e. the
16 biosphere, from fossil fuel and from biofuel burning are traced separately. Using the modelled mole
17 fractions and isotope records of CO₂, CO, $\delta^{13}\text{C}(\text{CO}_2)$ and $\Delta^{14}\text{C}(\text{CO}_2)$, we estimate the total fuel
18 CO₂ offset using these tracers. We then discuss advantages and disadvantages of the different
19 tracers. Using a modelled data set has the additional advantage, that isotopic signatures, emission
20 ratios of different emission sectors etc. can be varied in order to also investigate the sensitivity of
21 these source characteristics on the fuel CO₂ estimate. This enables us to judge how accurately the
22 sources in the catchment of the measurement site need to be characterized for a certain required
23 accuracy of fuel CO₂, and if a calibration, using e.g. precise $\Delta^{14}\text{C}(\text{CO}_2)$ measurements, is
24 advantageous. In the course of this, we also compare different possible sampling strategies for
25 calibration. We further assess, which measurement precision is needed to achieve continuous fuel
26 CO₂ estimates with sufficient precision. Additionally, we investigate the diurnal cycle of the tracer-
27 based continuous fuel CO₂ estimates and compare them to the modelled reference fuel CO₂ in order
28 to determine if we can reproduce the diurnal cycle correctly and hence, if we would introduce
29 significant biases when using e.g. only afternoon values of fuel CO₂ in inverse models.

30 We discuss the model results for a three typical European sites with different degrees of pollution,
31 which differ in their annual mean fuel CO₂ offset. We define three pollution regimes, which we

1 call “rural”, “urban” and “polluted”. Rural sites have mean fuel CO₂ offsets of 0-5 μmol/mol. We
2 here use the (hypothetical) station Gartow (53°0’ N, 11°3’ E) as example with a mean fuel CO₂
3 offset of 3 μmol/mol. Gartow is located in Northern Germany about 160 km north-west of Berlin.
4 Urban sites span a range from 5-20 μmol/mol. We exemplary use Heidelberg, which is a typical
5 urban measurement site with large fuel CO₂ emissions, but also similarly high biogenic sources
6 and sinks in the catchment, which are also active during relatively mild winters. The mean modelled
7 fuel CO₂ offset in Heidelberg is about 16 μmol/mol (24 hours). Polluted sites exhibit annual mean
8 fuel CO₂ offsets larger than 20 μmol/mol. A station in the outskirts of Berlin (52°5’ N, 13°6’ E) is
9 used as example site with modelled mean fuel CO₂ offset of 25 μmol/mol). For all sites, we looked
10 at the same height above ground level (30m a.g.l). Note, that this classification relates only to the
11 mean annual offset and not to single pollution events. We assess, if an estimation of continuous
12 fuel CO₂ is possible at all sites and what may be the best tracer. Finally, we give an outlook on how
13 to apply this model study to a real measured data set. Our investigation aims at providing the basis
14 for the decision if continuous measurements of CO₂, CO, δ¹³C(CO₂) and Δ¹⁴C(CO₂) would be
15 worth to conduct at a particular measurement station in order to quantitatively and precisely
16 estimate continuous fuel CO₂ within a measurement network.

17

18 **2. The modelling framework**

19 For the study’s purpose of theoretically assessing precision and accuracy of different tracer
20 configurations for fuel CO₂ estimation, it is only of secondary importance that modelled time series
21 are correct, but it is mainly important that the model provides a reasonably realistic data set. In this
22 study, we simulate mole fractions and isotopic records for the Heidelberg site (49°3’ N, 8°4’ E,
23 urban, see Levin et al., 2003) and for two non-existing stations Gartow (53°0’ N, 11°3’ E, rural)
24 and Berlin (52°5’ N, 13°6’ E, polluted) for the year 2012. All three stations may potentially be part
25 of the German ICOS atmospheric network (see <http://www.icos-infrastructure.eu/>).

26 We used the Stochastic Time-Inverted Lagrangian Transport (STILT) model (Lin et al., 2003) as
27 well as pre-set source and sink distributions (see below). To simulate the atmospheric transport we
28 used meteorological fields from the European Center for Medium-Range Weather Forecast with 3-
29 hourly temporal resolution and 25 km x 25 km spatial resolution (Trusilova et al., 2010). Details
30 of the STILT model are given in Lin et al. (2003) and in Gerbig et al. (2003); here we only provide

1 a few relevant details. By emitting 100 particles (representing the observed air parcel) at the
2 measurement location and time and inverting the meteorological fields in time, it is possible to
3 follow the particles' trajectories backward in time using mean wind and a parameterization for the
4 turbulent motion. For each of the trajectories, the sensitivity to emission fluxes is derived based on
5 the residence time within the lower half of the mixed layer during each advection time step
6 (typically 0.25 to 1 hours). The sensitivity of the observed tracer mole fraction to upstream
7 emissions was derived by combining the sensitivities of each trajectory on a common horizontal
8 grid (here $1/12^\circ$ latitude x $1/8^\circ$ longitude, corresponding to about 10 km x 10 km). To reduce impact
9 from undersampling of upstream areas at times when particles are distributed over extensive areas
10 with large gaps between neighboring particles, the effective horizontal size of the grid cells is
11 increased dynamically with increasing separation of the particles (Gerbig et al., 2003). This allows
12 efficient simulations with a relative small ensemble size. The sensitivity of the mole fraction at the
13 measurement site to emissions located upstream is typically called footprint. The particles are
14 traced back in time until they leave the model domain, which extends from 16°W to 36°E and from
15 32°N to 74°N . Initial/lateral CO_2 tracer boundary conditions for CO_2 tracer far-field mole fractions
16 are taken from analyzed CO_2 fields, generated by the global atmospheric tracer transport model,
17 TM3 (Heimann and Körner, 2003), based on optimized fluxes (Rödenbeck, 2005) transported at a
18 spatial resolution of $4^\circ \times 5^\circ$ with 19 vertical levels, and a temporal resolution of 6 hours (s96 v3.6,
19 <http://www.bgc-jena.mpg.de/~christian.roedenbeck/download-CO2-3D/>). The footprint is
20 multiplied with the biospheric and anthropogenic surface emissions to estimate the mole fraction
21 change at the measurement site.

22 For the biospheric CO_2 fluxes, we use the vegetation photosynthesis and respiration model (VPRM,
23 Mahadevan et al., 2008). The Net Ecosystem Exchange is calculated for different biome types
24 based on SYNMAP (Jung et al., 2006) using land surface water index and enhanced vegetation
25 index from MODIS (<http://modis.gsfc.nasa.gov/>) satellite data, as well as air temperature and short
26 wave radiation from ECMWF. VPRM results are computed at $1/12^\circ \times 1/8^\circ$ resolution with hourly
27 resolution. We neglect biospheric CO and CH_4 fluxes in the model. CO destruction by OH and CO
28 production via CH_4 oxidation is taken into account (Gerbig et al., 2003). However, CO production
29 via non-methane hydrocarbon (NMHC) oxidation and CO uptake by soils (Conrad, 1996) are not
30 included in the model. When using CO as tracer for fuel CO_2 , neglecting natural CO sources and

1 sinks may be problematic since natural sources would lead to an overestimation and natural sinks
 2 to an underestimation of fuel CO₂. We will discuss this in more detail in Sect. 3.3.2 and 3.4.

3 Anthropogenic emissions of CO₂, CO and CH₄ are from a preliminary version of the EDGARv4.3
 4 emission inventory (EC-JRC/PBL, 2015), also used for the UNEP Emissions Gap Report (Rogelj
 5 et al., 2014) for the base year 2010 and have a spatial resolution of 0.1° x 0.1°. The emissions are
 6 further separated following IPCC emission categories, which are again separated in fuel types (i.e.
 7 hard coal, brown coal, oil, natural gas, derived gas, biofuels etc.). To extrapolate the emissions to
 8 the year 2012 specifically we follow the approach taken in the COFFEE dataset (CO₂ release and
 9 Oxygen uptake from Fossil Fuel Emission Estimate) (Steinbach et al., 2011) and use specific
 10 temporal factors (seasonal, weekly and daily cycles) (Denier van der Gon et al., 2011) for different
 11 emission categories, and apply country and fuel type specific year-to-year changes at national level
 12 taken from the BP statistical review of World Energy 2014 (available at:
 13 [http://www.bp.com/en/global/corporate/about-bp/energy-economics/statistical-review-of-world-](http://www.bp.com/en/global/corporate/about-bp/energy-economics/statistical-review-of-world-energy.html)
 14 [energy.html](http://www.bp.com/en/global/corporate/about-bp/energy-economics/statistical-review-of-world-energy.html)).

15 The STILT model calculates the total trace gas mole fraction of CO₂ (y_{tot}) at the measurement site
 16 as the sum of a background mole fraction y_{bg} , contributions from the biosphere y_{bio} , from different
 17 fossil fuel types $y_{\text{ff},i}$ and different biofuel types $y_{\text{bf},j}$:

$$19 \quad y_{\text{tot}} = y_{\text{bg}} + y_{\text{bio}} + \sum_i y_{\text{ff},i} + \sum_j y_{\text{bf},j}$$

18 (1)

20 The last two terms of Eq. (1) form the total fuel CO₂ (y_{F}). We can associate a total isotopic
 21 $\delta^{13}\text{C}(\text{CO}_2)$ (δ_{tot}) record to the total CO₂ record following Mook (2001):

$$23 \quad \delta_{\text{tot}} y_{\text{tot}} \approx \delta_{\text{bg}} y_{\text{bg}} + \delta_{\text{bio}} y_{\text{bio}} + \sum_i \delta_{\text{ff},i} y_{\text{ff},i} + \sum_j \delta_{\text{bf},j} y_{\text{bf},j}$$

22 (2)

24 The isotopic signatures attributed to the different emission types, e.g. $\delta_{\text{ff},i}$ and δ_{bio} are listed in
 25 Table 1. Note that we do not implement a diurnal cycle into the biospheric signature.

1 The total CO mole fraction (x_{tot}) can be balanced in analogy to CO₂, but we neglect biospheric CO
 2 contributions as they are expected to be small:

$$4 \quad x_{\text{tot}} = x'_{\text{bg}} + \sum_i x_{\text{ff},i} + \sum_j x_{\text{bf},j} = x'_{\text{bg}} + \sum_i \frac{y_{\text{ff},i}}{\overline{R}_{\text{ff},i}} + \sum_j \frac{y_{\text{bf},j}}{\overline{R}_{\text{bf},i}} \quad (3)$$

5 The emission ratios $\overline{R}_{\text{ff},i}$ ($=\Delta x/\Delta y_{\text{ff},i}$) depend on the emission category as well as fuel type and are
 6 determined by the emission characteristics (implied emission factors) given in EDGARv4.3. The
 7 footprint-weighted mean ratios, e.g. \overline{R}_{F} , are listed in Table A1 for Heidelberg. For the background
 8 values $\Delta^{14}\text{C}_{\text{bg}}$, y_{bg} , δ_{bg} and x'_{bg} , we use those mole fractions where CH₄ mole fractions reach a
 9 minimum value within two days. This is mainly the case in the afternoon when vertical mixing is
 10 strongest (for more details on the choice of background see appendix A2). Note, that the CO
 11 background x'_{bg} is denoted with a prime, since it has been corrected for chemical reactions with
 12 OH (sink) and for production from oxidation of CH₄ by applying a first-order chemical reaction on
 13 hourly OH and CH₄ fields. The contributions of fossil fuel and biofuel CO, are, however, not
 14 corrected for these chemical reactions in the model, since the CO, which is released in the footprint
 15 area of the measurement site typically travels only a fraction of its actual life-time until arriving at
 16 the measurement site.

17 The $\Delta^{14}\text{C}(\text{CO}_2)$ ($\Delta^{14}\text{C}_{\text{tot}}$) balance is also simulated and follows:

$$18 \quad y_{\text{tot}}(\Delta^{14}\text{C}_{\text{tot}} + 1) \approx y_{\text{bg}}(\Delta^{14}\text{C}_{\text{bg}} + 1) + y_{\text{bio}}(\Delta^{14}\text{C}_{\text{bio}} + 1) + \sum_i y_{\text{ff},i}(\Delta^{14}\text{C}_{\text{ff},i} + 1) + \\ 19 \quad \sum_j y_{\text{bf},j}(\Delta^{14}\text{C}_{\text{bf},j} + 1) \quad (4)$$

20 With $\Delta^{14}\text{C}_{\text{bio}}$, $\Delta^{14}\text{C}_{\text{bf},j}$ and $\Delta^{14}\text{C}_{\text{ff},i}$ listed in Table A1 and CO₂ mole fractions from model results. As
 21 all fossil fuel CO₂ sources are void of ¹⁴C(CO₂), fuel CO₂ contributions are separated into fossil
 22 fuel and biofuel contributions.

23 In the following, we use six different tracers or tracer combinations to derive continuous fuel CO₂:
 24 CO₂-only, CO, CO as tracer for traffic and $\delta^{13}\text{C}$ as tracer for all fuel CO₂ except that of traffic, CO
 25 as tracer for biofuel CO₂ and $\delta^{13}\text{C}(\text{CO}_2)$ as tracer for fossil fuel CO₂, $\delta^{13}\text{C}(\text{CO}_2)$ and $\Delta^{14}\text{C}(\text{CO}_2)$.
 26 The six tracer combinations were qualitatively motivated and described in the introduction and the
 27 equations are derived in the appendix A1, are summarized in Table 2. They are briefly appointed

1 here with their underlying assumptions: When using CO₂ as tracer for anthropogenic CO₂, we
2 assume that all CO₂ stems from anthropogenic sources and no biospheric sources or sinks exist in
3 the catchment area. In the CO-based method, we utilize that CO is co-emitted during anthropogenic
4 CO₂ emissions and assume that we know the monthly mean ratio of y_F to x_F . In the $\delta^{13}\text{C}(\text{CO}_2)$
5 approach, we use the isotopic depletion of fuel CO₂ relative to biospheric CO₂ and assume to know
6 the mean isotopic signature of fuel and biospheric CO₂. The $\Delta^{14}\text{C}(\text{CO}_2)$ -based approach makes
7 use of the fact that fossil fuel CO₂ contains no $^{14}\text{C}(\text{CO}_2)$ in contrary to biospheric (and biofuel)
8 $\Delta^{14}\text{C}(\text{CO}_2)$. Both need to be known for calculation. We also investigate the combination of CO
9 and $\delta^{13}\text{C}(\text{CO}_2)$, with CO as tracer for first, traffic CO₂ and second, biofuel CO₂ and $\delta^{13}\text{C}(\text{CO}_2)$ for
10 the respective remaining fuel CO₂. This separation was made, since in Europe traffic and biofuel
11 emissions both show a rather large ratio of CO/CO₂ compared to emissions from other sectors,
12 which makes CO a suitable tracer for these sectors. When separating between traffic and non-traffic
13 fuel CO₂, we need to know the monthly mean values for R_{tr} , m_{tr} , δ_{tr} and $\delta_{\text{F-tr}}$. This holds analogously
14 for separation between fossil fuel and biofuel CO₂. The different targeted emission groups (fuel
15 CO₂, fossil fuel CO₂, fuel CO₂ without traffic, traffic CO₂, biofuel CO₂ and biospheric CO₂) are
16 also listed and characterized in Table A1.

17
18

19 **3. Results**

20 We investigated how well the different tracer combinations perform at a typical urban, rural and
21 polluted measurement site. First, we will discuss the upper limit of precision and accuracy of fuel
22 CO₂ estimation using these tracers when assuming all parameters (e.g. $\overline{\delta_F}$) are known at every time
23 step. Here, the smallest possible time step is hours. We then investigate how the use of averaged
24 accurate parameters and variables affects the fuel CO₂ estimate. Next, we also perform a sensitivity
25 analysis to identify, which parameters and variables need to be known at which precision and
26 accuracy for fuel CO₂ estimation with satisfying accuracy (of e.g. better than 10%). Finally, we
27 discuss the diurnal variation of fuel CO₂ and include a realistic measurement uncertainty into our
28 considerations.

29

30 **3.1. High (hourly) resolution of parameters and variables**

1 The integrated footprint-weighted parameters (e.g. $\overline{R_F}$, $\overline{R_{tr}}$, $\overline{R_{bf}}$, $\overline{\delta_F}$, $\overline{\delta_{ff}}$, $\overline{\delta_{bf}}$, $\overline{\delta_{tr}}$, $\overline{\delta_{F-tr}}$, $\overline{m_{bf}}$ and
2 $\overline{m_{tr}}$) are needed for the estimation of fuel CO₂ using the tracers CO and $\delta^{13}\text{C}(\text{CO}_2)$ (see Appendix
3 A1 for derivation and Table 2 for summary of all equations). These parameters are dependent on
4 the emission characteristics of the sources in the catchment area of the measurement site. If e.g. the
5 mean isotopic signature of fuel CO₂ sources in the catchment area varies or if the catchment area
6 itself varies, the integrated footprint-weighted parameter $\overline{\delta_F}$ will change. Typically, the integrated
7 footprint-weighted parameters vary on time scales of hours, weeks, months and years. If, for a
8 given measurement site, we could determine these parameters on the time scale of hours (which is
9 the temporal resolution of our model), we would be able to estimate fuel CO₂ entirely correctly
10 (difference of estimated and modelled fuel CO₂ would be zero) using CO and $\delta^{13}\text{C}(\text{CO}_2)$ or any
11 combination of these tracers.

12 In contrast to methods using CO and/or $\delta^{13}\text{C}(\text{CO}_2)$, CO₂-only will overestimate fuel CO₂ when
13 biospheric CO₂ contributions are positive (which will often be the case during night time and in
14 winter) and underestimate fuel CO₂ when the biospheric CO₂ is negative (which may be the case
15 during daytime in summer). This leads to time-dependent biases depending on the proportion of
16 biospheric CO₂ to total CO₂ at the location, which is in general not negligible compared to the fuel
17 CO₂ signal.

18 As $\Delta^{14}\text{C}(\text{CO}_2)$ is not sensitive to biofuel contributions, $\Delta^{14}\text{C}(\text{CO}_2)$ based fuel CO₂ estimates will
19 underestimate the fuel CO₂ contributions approximately by the amount of biofuel CO₂ to the
20 regional CO₂ concentration offset. Additionally, any $^{14}\text{C}(\text{CO}_2)$ emissions from nearby nuclear
21 power plants or nuclear fuel reprocessing plants could potentially mask the depletion of fuel CO₂
22 contributions. Nuclear power plant emissions were not implemented in this model, but we will
23 shortly discuss their possible effects in Sect. 5.

24

25 **3.2. Low (monthly) resolution of parameters and variables**

26 Normally it will not be possible to determine parameters such as $\overline{R_F}$, $\overline{R_F}$, $\overline{R_{tr}}$, $\overline{R_{bf}}$, $\overline{\delta_F}$,
27 $\overline{\delta_{ff}}$, $\overline{\delta_{bf}}$, $\overline{\delta_{tr}}$, $\overline{\delta_{F-tr}}$, $\overline{m_{bf}}$ and $\overline{m_{tr}}$ with hourly resolution. We, thus, investigate how using monthly
28 median values of these parameters may influence the fuel CO₂ estimates. We will discuss later how
29 we can obtain their monthly mean values and, for now, assume they are known on a monthly basis.

1 We now only use the monthly median value of the footprint-weighted parameters $\overline{R_F}$, $\overline{R_F}$, $\overline{R_{tr}}$,
2 $\overline{R_{bf}}$, $\overline{\delta_F}$, $\overline{\delta_{ff}}$, $\overline{\delta_{bf}}$, $\overline{\delta_{tr}}$, $\overline{\delta_{F-tr}}$, $\overline{m_{bf}}$ and $\overline{m_{tr}}$ to estimate fuel CO₂. Note, that we use the median
3 instead of the mean value for the footprint-weighted parameters, since the median is less sensitive
4 to outliers. Using only monthly median values will introduce sub-monthly inaccuracies into the
5 fuel CO₂ estimate since the footprint-weighted parameters vary on sub-monthly timescales. The
6 variability of the discrepancy between estimated and reference (directly modelled) fuel CO₂
7 estimates will depend on the magnitude of sub-monthly variations of $\overline{R_F}$, $\overline{R_F}$, $\overline{R_{tr}}$, $\overline{R_{bf}}$, $\overline{\delta_F}$,
8 $\overline{\delta_{ff}}$, $\overline{\delta_{bf}}$, $\overline{\delta_{tr}}$, $\overline{\delta_{F-tr}}$, $\overline{m_{bf}}$ and $\overline{m_{tr}}$, but also on their absolute values. For example, the more
9 depleted the fuel CO₂ emissions are, the larger the isotopic difference between emissions from the
10 biosphere and from fuel burning and the better the tracer $\delta^{13}\text{C}(\text{CO}_2)$ will be for fuel CO₂ emissions
11 as both emission groups can be isotopically distinguished clearly (see Appendix C). For our model
12 setting, the sub-monthly variations (standard deviation) are about ± 3 (nmol/mol)/(μmol/mol) for
13 $\overline{R_F}$, $\overline{R_{tr}}$ and $\overline{R_{bf}}$, ± 0.2 (nmol/mol)/(nmol/mol) for $\overline{m_{bf}}$ and $\overline{m_{tr}}$, ± 2 ‰ for $\overline{\delta_F}$, $\overline{\delta_{ff}}$, $\overline{\delta_{bf}}$,
14 $\overline{\delta_{tr}}$ and $\overline{\delta_{F-tr}}$ (variations due to varying footprints in the STILT model and temporal emission
15 patterns of the different emission sectors). This variation is propagated into the fuel CO₂ estimate.
16 The corresponding distribution of the difference between the estimated and modelled fuel CO₂ can
17 be seen in Fig. 1 for the station Heidelberg.

18 The mean difference between the modelled and tracer-based fuel CO₂ estimate provides a measure
19 for the accuracy of the fuel CO₂ determination with the different tracer methods. In principle, one
20 cannot assume that, when using the correct median values for $\overline{R_F}$, $\overline{R_F}$, $\overline{R_{tr}}$, $\overline{R_{bf}}$, $\overline{\delta_F}$, $\overline{\delta_{ff}}$, $\overline{\delta_{bf}}$,
21 $\overline{\delta_{tr}}$ and $\overline{\delta_{F-tr}}$ no median bias will be introduced into the CO₂ estimate. The reason is that the
22 values for $\overline{R_F}$, $\overline{R_F}$, $\overline{R_{tr}}$, $\overline{R_{bf}}$, $\overline{\delta_F}$, $\overline{\delta_{ff}}$, $\overline{\delta_{bf}}$, $\overline{\delta_{tr}}$ and $\overline{\delta_{F-tr}}$ are calculated on an hourly basis
23 independent on the total fuel CO₂ value (y_F) at that time and are then averaged monthly. However,
24 if y_F and $\overline{R_F}$, $\overline{R_{tr}}$, $\overline{R_{bf}}$, $\overline{\delta_F}$, $\overline{\delta_{ff}}$, $\overline{\delta_{bf}}$, $\overline{\delta_{tr}}$ and $\overline{\delta_{F-tr}}$ are correlated, sub-monthly over- and
25 underestimation of y_F due to sub-monthly variation of $\overline{R_F}$, $\overline{R_F}$, $\overline{R_{tr}}$, $\overline{R_{bf}}$, $\overline{\delta_F}$, $\overline{\delta_{ff}}$,
26 $\overline{\delta_{bf}}$, $\overline{\delta_{tr}}$ and $\overline{\delta_{F-tr}}$ will not necessarily not average out. An analysis of the bias (difference between
27 modelled and tracer-based fuel CO₂ estimate; x-axis in Fig. 1-3) introduced when using monthly
28 median footprint-weighted parameters is therefore vital. The standard deviations of the Gaussian
29 fits to the difference distributions (Fig. 1-3) provide a measure for the precision of fuel CO₂
30 determination.

1 All methods using $\delta^{13}\text{C}(\text{CO}_2)$ and/or CO (Fig. 1b-e, 2b-e and 3b-e) are able to estimate fuel CO_2
2 without significant systematic biases, if the annual median parameters $\overline{\delta_{\text{ff}}}$, $\overline{\delta_{\text{bf}}}$, $\overline{\delta_{\text{tr}}}$, $\overline{\delta_{\text{F-tr}}}$ and $\overline{R_{\text{F}}}$
3 are known (see Sect. 3.3. for the case that they are not accurately known). Mean and median
4 differences of modelled and estimated fuel CO_2 are within 10 % of the annual mean fuel CO_2
5 signal. The benefit when using CO additionally to $\delta^{13}\text{C}(\text{CO}_2)$ is very small, which is due to the fact
6 that traffic or biofuel CO_2 contributions are not very distinct with respect to their isotopic signature
7 or their CO/ CO_2 emission ratio from the other fuel CO_2 contributions for our model settings. When
8 using CO as tracer for fuel CO_2 (Fig. 1b, 2b and 3b) the standard deviation of the difference
9 between the estimated and the true fuel CO_2 value is larger than when using $\delta^{13}\text{C}(\text{CO}_2)$. The reason
10 is the large sub-monthly variation of footprint-weighted $\overline{R_{\text{F}}}$ in our modelled data.

11 Generally, the absolute standard deviation of the different tracer distributions is larger at the
12 polluted station than at urban and rural stations. At the same time, we found that the variation of
13 the footprint-weighted parameters such as $\overline{R_{\text{F}}}$, $\overline{R_{\text{F}}}$, $\overline{R_{\text{tr}}}$, $\overline{R_{\text{bf}}}$, $\overline{\delta_{\text{F}}}$, $\overline{\delta_{\text{ff}}}$, $\overline{\delta_{\text{bf}}}$, $\overline{\delta_{\text{tr}}}$, $\overline{\delta_{\text{F-tr}}}$, $\overline{m_{\text{bf}}}$ and $\overline{m_{\text{tr}}}$
14 is largest in rural areas and smallest in polluted areas, which is probably due to the fact that in
15 polluted catchment areas the many polluters homogenize partly, whereas at cleaner sites the
16 emissions of the few different polluters are temporally and spatially distinct. Hence, the larger
17 spread of the fuel CO_2 estimate at polluted stations is not the result of larger source heterogeneity,
18 but is due to the larger absolute signals (and with that larger absolute variations) of fuel CO_2 in the
19 catchment area of these sites. Only CO_2 as tracer for fuel CO_2 shows less variability at the polluted
20 site Berlin, which is due to smaller contribution from the biosphere in its catchment area. However,
21 the relative variability ($=1\sigma/\text{mean}(y_{\text{F}})$) is significantly higher in Gartow (e.g. $\delta^{13}\text{C}$ -method: 20 %)
22 than it is in Heidelberg or Berlin (both ca. 5%). Differences and spreads of the CO_2 -only and
23 $^{14}\text{C}(\text{CO}_2)$ method were already described in Sect. 3.1.

24 We have found that only small median differences occur when using $\delta^{13}\text{C}(\text{CO}_2)$ or CO as tracer
25 for fuel CO_2 . This finding is only valid under the premise, that the median values of all input and
26 footprint-weighted parameters are known. If one or more of the parameters or variables are
27 assigned incorrectly, this will lead to a systematic error of the fuel CO_2 estimate. The sensitivity of
28 this misassignment for the different parameters and variables will be assessed in the next chapter.

29

30 **3.3. Sensitivity of fuel CO_2 estimates on misassigned parameters and variables**

1 We have investigated how well we are able to estimate fuel CO₂ in a setting in which e.g. the
2 monthly averages of all parameters are perfectly well known, but temporally varying on shorter
3 time scale. However, since, in reality, parameters such as $\overline{\delta_F}$ or $\overline{R_F}$ are only approximately known,
4 we need to investigate how a misassignment of one of these parameters will influence fuel CO₂
5 estimates. This will provide information on how well certain parameters and variables need to be
6 assigned for a fuel CO₂ estimate with targeted accuracy. For this purpose, we misassign one
7 parameter and, at the same time, keep the other parameters at their correct value. We then determine
8 how the fuel CO₂ estimate changes (y-axis in Fig. 4) when the misassignment of the parameter (x-
9 axis) varies. The sensitivities of all methods to the most important parameters and variables are
10 shown in Figure 4 exemplary for the urban site Heidelberg. We have done this analysis for the
11 parameters CO₂tot (Fig. 4a), $\delta^{13}\text{C}_{\text{tot}}$ (Fig. 4b), CO₂bg (Fig. 4c), $\delta^{13}\text{C}_{\text{bg}}$ (Fig. 4d), $\overline{\delta_F}$ (Fig. 4e), $\overline{\delta_{\text{bio}}}$
12 (Fig. 4f), $\overline{\delta_{\text{bf}}}$ (Fig. 4g), $\overline{\delta_{\text{tr}}}$ (Fig. 4h), CO offset (Fig. 4i), $\overline{m_{\text{bf}}}$, $\overline{m_{\text{tr}}}$ (Fig. 4j), $\overline{R_{\text{tr}}}$, $\overline{R_{\text{bf}}}$ (Fig. 4k),
13 $\overline{R_F}$ (Fig. 4l), $\Delta^{14}\text{C}_{\text{tot}}$ (Fig. 4m), $\Delta^{14}\text{C}_{\text{bg}}$ (Fig. 4n), $\Delta^{14}\text{C}_{\text{bio}}$ (Fig. 4o) and $\Delta^{14}\text{C}_{\text{bf}}$ (Fig. 4p). The variation
14 of these values was chosen in a way that the range includes the typical measurement precision for
15 CO₂meas, CO₂bg, δ_{bg} , δ_{meas} , $\Delta^{14}\text{C}_{\text{bg}}$ and $\Delta^{14}\text{C}_{\text{meas}}$. The variation of the CO offset was chosen in a way
16 that it displays the measurement precision of total CO and of the background CO, but also includes
17 realistic contributions from natural CO sources and sinks. For the parameters $\overline{R_F}$, $\overline{R_F}$, $\overline{R_{\text{tr}}}$, $\overline{R_{\text{bf}}}$, $\overline{\delta_F}$,
18 $\overline{\delta_{\text{ff}}}$, $\overline{\delta_{\text{bf}}}$, $\overline{\delta_{\text{tr}}}$, $\overline{\delta_{\text{F-tr}}}$, $\overline{m_{\text{bf}}}$, $\overline{m_{\text{tr}}}$, $\Delta^{14}\text{C}_{\text{bio}}$ and $\Delta^{14}\text{C}_{\text{bf}}$, we selected realistic ranges of sub-monthly
19 parameter variation.

20 The error bars given on the right hand side of Figure 4 show the interquartile ranges (IQR) and
21 stem from the sub-monthly variability of $\overline{\delta_F}$, $\overline{R_F}$, $\overline{m_{\text{bf}}}$ and $\overline{m_{\text{tr}}}$, which was discussed in chapter 3.2.
22 One can directly identify critical parameters and variables, for which the difference between the
23 modelled and estimated fuel CO₂ (y-axis) changes significantly with increasing misassignment of
24 parameters/variables (x-axis).

25

26 3.3.1 Sensitivity of CO₂-only method

27 We confirm that the CO₂-only method (green in Fig. 4) is insensitive to the variation of the
28 displayed parameters/variables.

29

1 3.3.2 Sensitivity of CO method

2 Critical parameters/variables of the CO method (orange in Fig. 4) are the CO offset ΔCO (Fig. 4i),
3 as well as the ratio \overline{R}_F ($=\Delta x/y_F$) (Fig. 4l). In practise, the CO offset is derived by subtracting the
4 CO background as well as natural CO source and sink contributions from the total measured CO
5 mole fraction. Typical fuel CO offsets are in the order of 40 nmol/mol. In our model we have not
6 included natural CO sources and sinks, but in practise, the uncertainty of the CO mole fraction
7 measurement and of the natural CO contributions will add to the uncertainty of the fuel CO₂
8 estimate. Assuming e.g. a CO background, which is 15 nmol/mol too large, or assuming an
9 additional sink resulting in a 15 nmol/mol lower CO background, which may be a realistic diurnal
10 variation of natural CO variation (Gros et al., 2002; Vogel, 2010), would lead to a significant
11 overestimation of fuel CO₂ of about 2.5 $\mu\text{mol/mol}$ (median). Therefore, for a real data set, it is vital
12 to determine the natural CO contributions and sinks (also soil sinks) using chemistry models or
13 calibration with e.g. $\Delta^{14}\text{C}(\text{CO}_2)$ (see Sect. 4). In Heidelberg, the median modelled ratio \overline{R}_F is about
14 5 ($\mu\text{mol/mol}$)/(nmol/mol) and shows a rather large variation of 3 (nmol/mol)/($\mu\text{mol/mol}$). Fig. 4l
15 shows, that such a variation of \overline{R}_F contributes significantly to the imprecision of fuel CO₂ in the
16 CO-method. Also, the correct determination of \overline{R}_F is vital for accurate fuel CO₂ estimates using
17 CO.

18

19 3.3.3 Sensitivity of methods using $\delta^{13}\text{C}(\text{CO}_2)$

20 The sensitivities of fuel CO₂ estimates using $\delta^{13}\text{C}(\text{CO}_2)$ only (blue in Fig. 4) and combinations of
21 $\delta^{13}\text{C}(\text{CO}_2)$ and CO are rather similar (red and black in Fig. 4). Note that the sensitivity on δ_{bg} or
22 δ_{tot} is plotted when keeping y_{bg} and y_{tot} constant. Changing the y_{bg} or y_{tot} values at the same time
23 when changing δ_{bg} or δ_{tot} (following a Keeling curve (Keeling, 1958; 1960) with typical mean $\delta^{13}\text{C}$
24 source of -25 ‰) results in about a factor ten smaller sensitivity and is therefore not critical.
25 However, small $\delta^{13}\text{C}(\text{CO}_2)$ variations (e.g. due to finite measurement precision or small
26 inaccuracies), which are uncorrelated with $\text{CO}_{2\text{tot}}$, lead to large biases in fuel CO₂, e.g. a
27 measurement bias of $\delta_{\text{tot}}=0.1$ ‰ leads to a fuel CO₂ misassignment of 5 ($\mu\text{mol/mol}$) (see Fig. 4b).
28 Therefore, a high measurement precision as well as accuracy of $\delta^{13}\text{C}(\text{CO}_2)$ is required for precise
29 and accurate fuel CO₂ estimation. Further critical parameters of the methods using $\delta^{13}\text{C}(\text{CO}_2)$ are
30 the isotopic signature of fuel CO₂ and the isotopic signature of biospheric CO₂ in the footprint (see

1 Fig. 4e, f). The isotopic signatures of fuel and biospheric CO₂ must therefore be well known (or
2 potentially calibrated, see Sect. 4), if we want to use $\delta^{13}\text{C}(\text{CO}_2)$ as tracer for fuel CO₂. Especially
3 assuming more enriched fuel isotopic signatures or too depleted biospheric signatures biases the
4 fuel CO₂ estimates strongly, because in these cases, biospheric and fuel CO₂ sources are difficult
5 to distinguish using $\delta^{13}\text{C}(\text{CO}_2)$.

6

7 3.3.4 Sensitivity of $\Delta^{14}\text{C}(\text{CO}_2)$ method

8 Figures 4 m-p display the sensitivity of the $\Delta^{14}\text{C}(\text{CO}_2)$ based estimate of fuel CO₂ on the variables
9 $\Delta^{14}\text{C}_{\text{tot}}$, $\Delta^{14}\text{C}_{\text{bg}}$ and $\Delta^{14}\text{C}_{\text{bio}}$. While fuel CO₂ is rather insensitive against misassignment of
10 $\Delta^{14}\text{C}(\text{CO}_2)_{\text{bio}}$ (Fig. 4o) and $\Delta^{14}\text{C}(\text{CO}_2)_{\text{bf}}$ (Fig. 4p), it is very sensitive on $\Delta^{14}\text{C}(\text{CO}_2)_{\text{tot}}$ (Fig. 4m) and
11 $\Delta^{14}\text{C}(\text{CO}_2)_{\text{bg}}$ (Fig. 4n) as was already described in Turnbull et al. (2007). Thus, precise and accurate
12 $\Delta^{14}\text{C}(\text{CO}_2)$ measurements are important for fuel CO₂ determination. Note, that the best currently
13 achieved measurement precision of conventional counting or AMS measurements is $\pm 2\%$
14 (equivalent to about $\pm 1.0 \mu\text{mol/mol}$ fuel CO₂), but the hypothetical future continuous GC-AMS
15 measurements may be of order $\pm 5\%$ (equivalent to about $\pm 3 \mu\text{mol/mol}$ fuel CO₂). The reason why
16 the fuel (biofuel + fossil fuel) CO₂ estimate based on ^{14}C is biased by about $1.1 \mu\text{mol/mol}$ is due to
17 the fact that biofuel CO₂, in contrast to fossil fuel CO₂, contains $^{14}\text{C}(\text{CO}_2)$ and is therefore not
18 detectable by lack of $^{14}\text{C}(\text{CO}_2)$.

19

20 3.4 Measurement precision and sub-monthly variation of parameters/variables

21 In Sect. 3.3.1-3.3.4, we have seen how sensitive the fuel CO₂ estimates are to the total mole
22 fractions and δ/Δ -values. Since they have a large impact on the fuel CO₂ estimate, we now include
23 their uncertainty into our analysis of precision of fuel CO₂ estimation. In order to display the effect
24 of a limited measurement precision of CO₂, CO, $\delta^{13}\text{C}(\text{CO}_2)$ and $\Delta^{14}\text{C}(\text{CO}_2)$ we construct random
25 realizations with mean value zero and a specific standard deviation. Additionally, we add a random
26 variation to the CO offset and the biospheric/biofuel isotopic (δ/Δ -) signature in order to simulate
27 the effect of variability of CO to CO₂ ratio and of isotopic end members. These random
28 uncertainties were not included in Sec 3.1 and 3.2 and in Fig. 1-3. Note, that in reality these
29 variations may not be randomly distributed. E.g. we may introduce a systematic bias in one

1 direction if we have unaccounted production of CO from VOCs or, if we have unaccounted CO
2 (e.g. soil) sinks. These sources and sinks will not occur randomly, but have a distinct sub-monthly
3 pattern. Depending on the sign of the net natural CO flux, the bias may be positive or negative.
4 However, for simplicity, we also include the natural CO variation here as a random vector as no
5 natural CO sinks or sources are included in the modelled CO offset, but we want to show the
6 possible effect of their variation.

7 The random vectors, which were used in this study are summarized in Table 3 with their magnitude
8 being motivated. The distributions of the difference between estimated (incl. measurement and
9 parameter uncertainties and sub-monthly variations) and modelled fuel CO₂ can be seen in Fig. 5-
10 7. Note that a possible misassignment of parameters or variables as investigated in Fig. 4 is neither
11 accounted for in Fig. 1-3 nor in Fig. 5-7.

12 When including the measurement uncertainties and (input and footprint-weighted) parameter
13 variability into the considerations, the mean bias remains unaltered, since the included uncertainty
14 is random. However, the distributions of the CO and $\delta^{13}\text{C}(\text{CO}_2)$ -based approaches for rural sites
15 (such as Gartow), medium polluted sites (such as Heidelberg) and polluted sites (such as Berlin)
16 widen significantly by about the same amount for all three sites. This is due to identical assumed
17 measurement precisions and parameter variations. Since the absolute fuel CO₂ offset is larger in
18 Berlin (annual modelled average ca. 25 $\mu\text{mol}/\text{mol}$), than in Heidelberg (16 $\mu\text{mol}/\text{mol}$), and in
19 Gartow (3 $\mu\text{mol}/\text{mol}$), the relative variability ($=1\sigma/\text{mean}(y_F)$) is smallest for the measurement site
20 in Berlin (e.g. ca. 15 % for $\delta^{13}\text{C}(\text{CO}_2)$ -method) and largest for Gartow (110 % for $\delta^{13}\text{C}(\text{CO}_2)$ -
21 method). At present, it is therefore questionable whether the estimation of continuous fuel CO₂ is
22 at rural measurement sites. Even $\Delta^{14}\text{C}(\text{CO}_2)$ measurements with a precision of 5 ‰ result in a
23 variability in fuel CO₂ of 60%, but a $\Delta^{14}\text{C}(\text{CO}_2)$ precision of 2 ‰ would lead to a variability in
24 fuel CO₂ of only 35% at rural sites (not shown here). The reduced precision of fuel CO₂ estimates,
25 which we observe when including limited measurement precision into our considerations,
26 highlights again the necessity of performing precise atmospheric measurements of $\delta^{13}\text{C}(\text{CO}_2)$ and
27 CO₂ if we want to use $\delta^{13}\text{C}(\text{CO}_2)$ as tracer for fuel CO₂.

28 For urban sites, CO and $\delta^{13}\text{C}(\text{CO}_2)$ -based methods show a very similar precision of about 4
29 $\mu\text{mol}/\text{mol}$ (1σ). At urban sites, $\delta^{13}\text{C}(\text{CO}_2)$ is slightly more precise than CO. It is worth pointing out
30 that CO₂-only may be an adequate tracer for fuel CO₂ in polluted areas in the winter time as

1 absolute biases are small (<4%) and the precision (ca. 12 %) is rather good. $\Delta^{14}\text{C}(\text{CO}_2)$
2 measurements with a precision of 5 ‰ would be the best tracer at all stations, but is currently not
3 available yet.

4 5 **3.5. Comparison of the estimated fuel CO₂ diurnal cycle with different tracer** 6 **configurations**

7 As the diurnal cycle of CO₂ emissions is coupled to a diurnal change of the atmospheric mixing
8 layer height, fuel CO₂ mole fraction varies during the day. In our calculations, we only use monthly
9 median values of $\overline{R_F}$, $\overline{R_F}$, $\overline{R_{tr}}$, $\overline{R_{bf}}$, $\overline{\delta_F}$, $\overline{\delta_{ff}}$, $\overline{\delta_{bf}}$, $\overline{\delta_{tr}}$, $\overline{\delta_{F-tr}}$, $\overline{m_{bf}}$ and $\overline{m_{tr}}$ for fuel CO₂ estimation.
10 Discrepancies between the modelled reference diurnal cycle and the tracer based diurnal cycle may
11 be introduced due to a diurnal cycle of the parameters $\overline{R_F}$, $\overline{R_F}$, $\overline{R_{tr}}$, $\overline{R_{bf}}$, $\overline{\delta_F}$,
12 $\overline{\delta_{ff}}$, $\overline{\delta_{bf}}$, $\overline{\delta_{tr}}$, $\overline{\delta_{F-tr}}$, $\overline{m_{bf}}$ and $\overline{m_{tr}}$. We thus need to test if we are able to reproduce the diurnal fuel
13 CO₂ pattern in order to estimate fuel CO₂ from tracers at sub-diurnal resolution. Therefore, we
14 calculate the median diurnal fuel CO₂ cycles with the different methods and compare them to the
15 reference model diurnal cycle for summer and for winter (see Fig. 8 exemplary for the urban station
16 Heidelberg).

17 One can see that the $\delta^{13}\text{C}(\text{CO}_2)$ method reproduces the reference diurnal cycle within its variability
18 very well (standard errors of the respective hour in a half year are denoted as error bars in Fig. 8).
19 Median hourly differences are about 0.1 ± 0.7 $\mu\text{mol/mol}$ for methods using $\delta^{13}\text{C}(\text{CO}_2)$. The CO₂-
20 only method largely overestimates fuel CO₂ contributions during the night by up to 10 $\mu\text{mol/mol}$
21 in winter and by about 15-25 $\mu\text{mol/mol}$ in summer. During the afternoon, the CO₂-only method
22 overestimates fuel CO₂ in winter and underestimates it in summer. Even though the absolute
23 difference is small during the afternoon, the relative difference is still large. The CO₂-only method
24 is therefore not able to trace the diurnal fuel CO₂ variation at a site like Heidelberg correctly. Using
25 $\Delta^{14}\text{C}(\text{CO}_2)$ for fuel CO₂ estimation leads to a slight median underestimation throughout the day
26 (and season), which is due to the presence of $^{14}\text{C}(\text{CO}_2)$ in biofuel CO₂ masking all biofuel CO₂
27 contributions. The CO-method slightly overestimates fuel CO₂ during nighttime by about 10% in
28 winter and 20 % in summer. The standard deviation of the hourly medians of the differences
29 between model and CO-based fuel CO₂ is about 15 % of the total fuel CO₂.

1 One could consider implementing a diurnal correction into the fuel CO₂ estimate in a way that not
2 only monthly median values of $\overline{R_F}$, $\overline{R_{tr}}$, $\overline{R_{bf}}$, $\overline{\delta_F}$, $\overline{\delta_{ff}}$, $\overline{\delta_{bf}}$, $\overline{\delta_{tr}}$, $\overline{\delta_{bio}}$, $\overline{\delta_{F-tr}}$, $\overline{m_{bf}}$ and $\overline{m_{tr}}$ are used, but
3 also hourly correction factors for these parameters are multiplied (c.f. Vogel et al. 2010). This will
4 be advantageous if the parameters exhibit a significant diurnal cycle themselves. However, for our
5 setting, implementing a diurnal correction factor only slightly improves the agreement between the
6 model and the estimated fuel CO₂ (not shown here). The reason is that the (hourly) median
7 footprint-weighted parameters do not influence the (hourly) median fuel CO₂ estimates linearly,
8 and that the synoptic variations of the footprint-weighted parameters are larger than the diurnal
9 variations. Therefore, an hourly median correction factor does not necessarily improve the hourly
10 fuel CO₂ estimate. We note that no diurnal systematic variability of the isotopic biospheric
11 (respiration and photosynthesis) signature as well as of the non fuel CO sinks and sources (which
12 would be treated as an enhancement or reduction of the CO offset ΔCO) were implemented, but
13 only random uncertainties of ± 2 ‰ for δ_{bio} and ± 15 nmol/mol for ΔCO . This assumption of
14 random variability will not be correct, if systematic (e.g. diurnal) variation of $\delta^{13}C_{bio}$ and non fossil
15 ΔCO variation occur. For $\delta^{13}C_{bio}$ the diurnal changes are expected to be small (<1 ‰ (Flanagan et
16 al., 2005) corresponding to fuel CO₂ biases of <0.5 $\mu\text{mol/mol}$), but for CO these may be larger
17 (e.g. diurnal natural ΔCO variation of about 10 nmol/mol may occur from dry deposition of CO in
18 forest soils during night and from photochemical production of CO by hydrocarbons during the
19 day (Gros et al., 2002) corresponding to ca. 2.5 $\mu\text{mol/mol}$ fuel CO₂). Therefore, in a real setting, it
20 might be necessary to model natural CO concentration in order to not introduce a bias into diurnal
21 y_F structures.

22 In inverse model studies, often only afternoon hours are used to derive fluxes, as the atmospheric
23 mixing can be better simulated by the models during conditions with a well developed mixed layer
24 (Gerbig et al., 2008). Therefore, it is especially important to check the afternoon values of fuel
25 CO₂. Figure 8 shows an enlarged inlay of the diurnal cycle during the afternoon hours. Since in
26 this model study we use the minimum of total CH₄ values within two days as background value
27 (Appendix A2), the afternoon offsets are very small, leading to a low signal to noise ratio. However,
28 differences between the $\delta^{13}C(\text{CO}_2)$, CO, and $\Delta^{14}C(\text{CO}_2)$ -based and reference fuel CO₂ are very
29 small as well (mean differences <10 % of afternoon fuel CO₂ value, standard deviation of
30 differences about 30%). Therefore, it seems justified to use an ensemble of afternoon values of

1 continuous fuel CO₂ estimates (based on $\delta^{13}\text{C}(\text{CO}_2)$ or CO) for inverse model studies despite the
2 small absolute fuel CO₂ values of about 1-2 $\mu\text{mol}/\text{mol}$ in the afternoon hours at an urban site.

3

4 **4. Calibration of $\overline{\delta_F}$, $\overline{\delta_{F-tr}}$, $\overline{\delta_{ff}}$ and $\overline{R_F}$ with $\Delta^{14}\text{C}(\text{CO}_2)$ measurements**

5 In order to estimate fuel CO₂ accurately with methods using CO and/or $\delta^{13}\text{C}(\text{CO}_2)$, the parameters
6 $\overline{\delta_F}$, $\overline{\delta_{F-tr}}$, $\overline{\delta_{ff}}$ (and δ_{bio}) and $\overline{R_F}$ need to be known with high accuracy, since otherwise biases are
7 introduced into the fuel CO₂ estimate (see Fig. 4). However, for the evaluation of a measured data
8 set, $\overline{\delta_F}$, $\overline{\delta_{F-tr}}$, $\overline{\delta_{ff}}$, δ_{bio} and $\overline{R_F}$ are not per se available, but require either extensive source sampling
9 campaigns or good bottom-up inventories. Alternatively, these parameters could also be
10 “calibrated” using fossil fuel CO₂ estimates from $\Delta^{14}\text{C}(\text{CO}_2)$ measurements with high precision (in
11 addition to biofuel contributions, which need to be added on top). For this purpose, Eq. (1) and (2)
12 can be re-arranged and solved for calibration of $\overline{\delta_F}$, $\overline{\delta_{F-tr}}$, $\overline{\delta_{ff}}$ or $\overline{R_F}$ (for derivation see Appendix
13 B).

14 Since $\Delta^{14}\text{C}(\text{CO}_2)$ measurements are time-consuming and costly, in practice only a limited number
15 of $\Delta^{14}\text{C}(\text{CO}_2)$ measurements can be regularly performed. For example, in the Integrated Carbon
16 Observation System (ICOS) atmospheric network, the radiocarbon measurement capacity was
17 designed for about 50 radiocarbon measurements per station per year of which about 26 will be
18 used for integrated sampling for long-term monitoring of fossil fuel CO₂.

19 Previous radiocarbon calibration approaches suggested integrated (e.g. monthly) sampling of
20 $\Delta^{14}\text{C}(\text{CO}_2)$ for CO tracer calibration (cf. Levin and Karstens (2007) and Vogel et al., (2010) for
21 $\overline{R_F}$). Another possible approach for tracer calibration is to take grab samples rather than integrated
22 samples (e.g. Turnbull et al., 2011). Grab samples could be taken through-out the year and the
23 derived parameters $\overline{R_F}$ and $\overline{\delta_F}$, $\overline{\delta_{F-tr}}$, $\overline{\delta_{ff}}$ could then be averaged to one median value or separated
24 into seasons and averaged to separate values e.g. for summer and winter. The optimal sampling
25 strategy depends on the structure, variation and noise of $\overline{R_F}$ and $\overline{\delta_F}$, $\overline{\delta_{F-tr}}$, $\overline{\delta_{ff}}$ within one year.
26 Principally, it would also be possible to take all the samples consecutively at 2 hour intervals during
27 a so-called “event” and calculate the median value from the event. Therefore, we compare here
28 four different sampling strategies for parameter calibration, all using a total of n samples per year

1 (in ICOS: $n \approx 24$). Note that we include sub-monthly variation into the parameters and measurement
2 uncertainties into the observations (as in Sect 3.4).

3
4 1. Integrated sample calibration: Take $n/24$ integrated samples each month and their
5 associated background samples (for $n \approx 24$ that makes 12 monthly samples and 12
6 monthly background samples a year) and calibrate $\overline{R_F}$ and $\overline{\delta_F}$, $\overline{\delta_{F-tr}}$, $\overline{\delta_{ff}}$ on a monthly
7 basis from the integrated samples (this corresponds to the approach suggested by Levin
8 and Karstens (2007) and Vogel et al., (2010) for $\overline{R_F}$). In this approach, the mean ΔCO
9 and fuel ΔCO_2 (from integrated CO and $\Delta^{14}C(CO_2)$ sampling) over the course of one
10 month are used to calculate monthly $\frac{\langle \Delta x \rangle}{\langle \Delta y_F \rangle}$. However, since actually the mean of ratio $\overline{R_F}$
11 $= \langle \frac{\Delta x}{\Delta y_F} \rangle$ is required, and not the ratio of means $\frac{\langle \Delta x \rangle}{\langle \Delta y_F \rangle}$ (Vogel et al., 2010), biases may be
12 introduced into the fuel CO_2 estimate (same holds for the factors in $\overline{\delta_F}$, $\overline{\delta_{F-tr}}$ and $\overline{\delta_{ff}}$).

13
14 2. Annual grab sample calibration: Randomly select a number of samples $n/2$ (and their
15 associated afternoon background ($n/2$)) each year and calibrate annual median
16 $\overline{R_F}$ and $\overline{\delta_F}$, $\overline{\delta_{F-tr}}$, $\overline{\delta_{ff}}$. Biases introduced by this sampling strategy are twofold; first, the
17 random choice of grab samples may not represent the median annual value. This
18 potential bias decreases with increasing number of grab samples used. Second, the
19 potential seasonal cycle of the parameters is not considered. Therefore, in the annual
20 grab sample calibration, the winter-time and summer-time fuel CO_2 estimates will
21 always be shifted against each other, if $\overline{R_F}$ and $\overline{\delta_F}$, $\overline{\delta_{F-tr}}$, $\overline{\delta_{ff}}$ exhibit a seasonal cycle, but
22 only one annual median value for these parameters would be used.

23
24 3. Seasonal grab sample calibration: Randomly select a number of samples $n/4$ (and their
25 associated afternoon background ($n/4$)) in summer and in winter and calibrate a median
26 $\overline{R_F}$ and $\overline{\delta_F}$, $\overline{\delta_{F-tr}}$, $\overline{\delta_{ff}}$ with half-yearly resolution. Here again, the random choice of grab
27 samples may not represent the median half annual value, and a potential bias may be
28 even larger here than in the annual grab sample calibration, since only half the samples
29 are available to obtain a robust value for $\overline{R_F}$ and $\overline{\delta_F}$, $\overline{\delta_{F-tr}}$, $\overline{\delta_{ff}}$ for summer and winter.

1 In return, it is principally possible to detect the seasonal variation of
2 $\overline{R_F}$ and $\overline{\delta_F}$, $\overline{\delta_{F-tr}}$, $\overline{\delta_{ff}}$.

- 3
- 4 4. Seasonal event calibration: Randomly select an “event day” each season. On this day,
5 select $n/2-2$ consecutive grab samples (and 1 associated afternoon background) and
6 calibrate a median $\overline{R_F}$ and $\overline{\delta_F}$, $\overline{\delta_{F-tr}}$, $\overline{\delta_{ff}}$ with half-yearly resolution. This approach is
7 similar to approach 3, but entails a greater risk of choosing an event, which is not
8 representative for the entire season, since subsequent samples are not independent of
9 each other. On the other hand, it has the advantage of using more calibrations for the
10 same number of radiocarbon measurements as approach 3 since only one background
11 sample is needed for each event. However, if the background sample is biased, it will
12 influence the entire event.

13

14 Comparing these sampling strategies to each other using one model run is difficult, since the result
15 changes from random realization to random realization, depending on the selection of calibration
16 samples in sampling strategy 2-4. We have therefore performed a Monte-Carlo simulation (with
17 500 runs) and used the root median square difference between the obtained and originally modelled
18 reference values $\overline{R_F}$ and $\overline{\delta_F}$, $\overline{\delta_{F-tr}}$, $\overline{\delta_{ff}}$ to calculate the difference between tracer-based estimate and
19 modelled reference fuel CO₂.

20 Table 4 shows the mean difference and standard deviation (as determined from a Gaussian fit to
21 the difference histogram of modelled and tracer-based fuel CO₂, in analogy to Fig. 5) for an urban
22 setting. One can see that the “integrated sample calibration” causes biases due to the covariance of
23 the factors in Eq. (B1) - (B4). The effect is much stronger for methods using $\delta^{13}C$ (ca. 15 % of
24 mean fuel CO₂ offset in Heidelberg (16 $\mu\text{mol/mol}$) than for the CO method (ca. 5 %). This bias is
25 directed meaning that it is not a random uncertainty, but actually a systematic bias introduced by
26 computation. This is different from the calibrations on grab samples, which have a bidirectional
27 absolute difference. Bidirectional differences may be advantageous over unidirectional differences
28 when analyzing long-term records as bi-directional differences contribute to long-term noise rather
29 than biases. For CO, it seems that the integrated calibration approach works well, but a uni-directed
30 bias remains. Note, that the differences found here are not due to the insensitivity of biofuel CO₂

1 contributions of $\Delta^{14}\text{C}(\text{CO}_2)$, as we add the (assumed as known) biofuel CO_2 prior to “calibration”
2 (see Eq. (B1)-(B3)).

3 We further find that since $\overline{\delta_{\text{F}}}$, $\overline{\delta_{\text{F-tr}}}$, $\overline{\delta_{\text{ff}}}$ and $\overline{R_{\text{F}}}$ do not exhibit a strong annual cycle, but show rather
4 large, high-frequent variations, the best sampling strategy for 24 available radiocarbon
5 measurements per year (as would be the case for the ICOS network) is using all available samples
6 to calibrate well-defined median annual values of $\overline{R_{\text{F}}}$ and $\overline{\delta_{\text{F}}}$, $\overline{\delta_{\text{F-tr}}}$, $\overline{\delta_{\text{ff}}}$ (sampling strategy 2). Only,
7 with 96 (or more) available radiocarbon measurements, it may be advisable to group the
8 calibrations into half-yearly intervals. Having such many radiocarbon grab samples available may
9 be a realistic scenario, if the parameters do not show any trend over the course of several years.
10 Note, that a monthly grab sample calibration (not shown here) results in large biases of about ± 3
11 $\mu\text{mol/mol}$ for CO -based as well as $\delta^{13}\text{C}(\text{CO}_2)$ -based methods and are thus, not advisable.

12 The accuracy of the seasonal event calibration is slightly worse than the accuracy of the seasonal
13 calibration (see Table 4) due to non-representativeness of a single event for the entire season.

14

15 **5. Discussion and Conclusion**

16

17 In this work, we analyzed the advantages and disadvantages of different tracers for estimating
18 continuous fuel CO_2 at different types of measurement stations. The accuracy and precision of
19 continuous fuel CO_2 estimates at three exemplary stations, one rural, one urban and one polluted
20 site were calculated. This should serve as orientation for the development of an atmospheric
21 measurement strategy, so that the best tracer configuration for a particular station can be chosen to
22 resolve the different CO_2 source components over a country or region. The results can be used to
23 plan and construct new measurement networks and sampling strategies with the goal of deriving
24 fuel CO_2 concentrations at high temporal resolution.

25 The results of our model study suggest that with our current measurement precision of continuous
26 tracers such as CO , $\delta^{13}\text{C}(\text{CO}_2)$ (or $\Delta^{14}\text{C}(\text{CO}_2)$), in general it is not possible to estimate fuel CO_2 at
27 rural areas ($5 \mu\text{mol/mol}$ or less of fuel CO_2) with a precision better than 100% (due to the small
28 signal to noise ratio). It could still be possible to monitor single pollution events since the signal
29 to noise ratio is much higher during such events. At present, it thus seems not helpful to equip

1 measurement stations in rural areas with continuous $\delta^{13}\text{C}(\text{CO}_2)$ and CO measurements with the
2 objective of monitoring continuous fuel CO_2 . However, it seems that tracer-based fuel CO_2
3 monitoring may be possible at urban or polluted sites (as e.g. planned within the Megacities Carbon
4 project) and may have the potential to improve the fuel CO_2 bottom-up inventories.

5 We find that CO_2 -only cannot be used as tracer for fuel CO_2 , as a significant contribution of CO_2
6 is released or taken up by the biosphere even in winter time. Only during winter in strongly polluted
7 areas, biogenic CO_2 contributions lead to a relatively small bias of about 5% with the CO_2 -only
8 approach and a small variation ($\sigma/\text{mean}(y_F)$): 5%, see Fig. 7).

9 In contrary to CO_2 -only, CO and $\delta^{13}\text{C}(\text{CO}_2)$ can be used as tracer for fuel CO_2 in summer and in
10 winter at urban and polluted sites. The accuracy of CO- and/or $\delta^{13}\text{C}(\text{CO}_2)$ -based fuel CO_2 estimates
11 depends to a large degree on how well the different parameters such as e.g. \overline{R}_F , $\overline{\delta}_F$, and δ_{bio} are
12 known. Missassignment leads to significant biases in the fuel CO_2 estimate (Fig. 4). Therefore, in
13 practice, it is important to screen and monitor all sources and sinks in the catchment area of the
14 measurement site and to determine the median isotopic source signature and the median ratios \overline{R}_F ,
15 \overline{R}_{tr} , \overline{R}_{bf} as well as the CO offset as accurately as possible, e.g. by calibration with co-located
16 $\Delta^{14}\text{C}(\text{CO}_2)$ measurements. The accuracy of the fuel CO_2 estimate after ^{14}C -calibration depends
17 strongly on the number of radiocarbon samples available for calibration and on the sampling
18 strategy used. E.g. In the ICOS project, approximately 24 radiocarbon samples will be available
19 for calibration of \overline{R}_F , $\overline{\delta}_F$, $\overline{\delta}_{\text{ff}}$, or $\overline{\delta}_{F-\text{tr}}$. With that amount of calibration samples available, due to
20 the large noise of the calibrated footprint-weighted parameters $\overline{\delta}_F$, $\overline{\delta}_{\text{ff}}$, or $\overline{\delta}_{F-\text{tr}}$ it may be
21 advantageous to group all calibrations to obtain robust annual median values for $\overline{\delta}_F$, $\overline{\delta}_{\text{ff}}$, or $\overline{\delta}_{F-\text{tr}}$.
22 If a large number of precise radiocarbon measurements are available or if the parameters do not
23 change over the course of several years and thus, several years of calibration samples can be
24 accumulated, it is advantageous to apply radiocarbon calibrations at half-yearly resolution. Note,
25 that due to changes in technology and technical processes, as well as due to a year-to-year variation
26 of extreme temperatures, the contribution from fuel CO_2 different sectors are likely to change
27 within a period of four years. However, this could be checked e.g. using night-time Keeling plot
28 intercepts (Vardag et al., in preparation). For calibration of \overline{R}_F , integrated $\Delta^{14}\text{C}(\text{CO}_2)$ calibration
29 could be used with rather small but systematic biases or grab samples could be used for slightly

1 larger, but random uncertainty. The accuracy then will typically be better than 10% for the CO-
2 method or the $\delta^{13}\text{C}(\text{CO}_2)$ method.

3 The precision of CO- and $\delta^{13}\text{C}(\text{CO}_2)$ -based approaches is very similar for all site classes, but for
4 polluted sites $\delta^{13}\text{C}(\text{CO}_2)$ seems slightly more precise. For Heidelberg it is about 25% (e.g.
5 $1\sigma/\text{mean}(y_F)$). For CO, the uncertainty originates mainly from the large variation of $\overline{R_F}$ in our
6 model runs due to the inhomogeneity of fuel CO sources in the footprint area of urban or polluted
7 measurement stations and due to natural CO sources. The uncertainty of the $\delta^{13}\text{C}(\text{CO}_2)$ approach
8 is mainly determined by the limited measurement precision of $\delta^{13}\text{C}(\text{CO}_2)$. Thus in order to use
9 $\delta^{13}\text{C}(\text{CO}_2)$ as a tracer for fuel CO_2 it is vital to perform isotopic measurements with a precision of
10 at least 0.05 ‰. The combination of $\delta^{13}\text{C}(\text{CO}_2)$ and CO for fuel CO_2 estimation is favorable in
11 cases where each of two emission groups is well distinguishable by one of the tracers. Since for
12 our model setting this is only partly the case (EDGAR emission inventory, see Table A1), the
13 combination of these tracers provides only little additional information.

14 We have found, that hypothetical future $\Delta^{14}\text{C}(\text{CO}_2)$ measurements with 5 ‰ absolute precision of
15 background and measured $\Delta^{14}\text{C}(\text{CO}_2)$ values (see Figure 5f-7f) would generally be a very precise
16 tracer for continuous fuel CO_2 estimation at rural ($1\sigma/\text{mean}(y_F) \approx 90\%$), urban (ca. 20%) and
17 polluted (ca. 10%) stations. The precision of fuel CO_2 estimates is determined mainly by the limited
18 measurement precision of background and total $\Delta^{14}\text{C}(\text{CO}_2)$ ($\pm 5\%$). Note however, that $\Delta^{14}\text{C}(\text{CO}_2)$
19 measurements with 5 ‰ precision are not yet fully developed and commercially available. For
20 comparison, a $\Delta^{14}\text{C}(\text{CO}_2)$ measurement precision of 1‰ would be needed to achieve a fuel CO_2
21 precision similar to that of $\delta^{13}\text{C}(\text{CO}_2)$ - and CO-based methods. An uncertainty of 2‰, which could
22 be a realistic near future precision of laser-based instruments (Galli et al., 2013), would lead to
23 relative uncertainties of 260%, 50% and 30% respectively. The downside of $\Delta^{14}\text{C}(\text{CO}_2)$ is its
24 inability to determine biofuel CO_2 . Therefore, the $\Delta^{14}\text{C}(\text{CO}_2)$ methods will underestimate the fuel
25 CO_2 (biofuel plus fossil fuel) contributions approximately by the share of biofuel in CO_2 at the site.
26 This may be only a small contribution as was the case for the studied year 2012 (e.g. 5% in
27 Heidelberg), but may increase in the future. Note also that we have not investigated the effect of
28 nuclear power plant $^{14}\text{C}(\text{CO}_2)$ contributions at the measurement site, which could additionally bias
29 fuel CO_2 estimates derived from $\Delta^{14}\text{C}(\text{CO}_2)$ measurements. Dispersion model results for
30 Heidelberg (pers. comm. Kuderer, 2015) suggest that the nuclear power facilities (most importantly

1 Philippsburg, located about 25 km south-west of Heidelberg), increase monthly mean $\Delta^{14}\text{C}(\text{CO}_2)$
2 by about $(2 \pm 2) \text{‰}$, corresponding to a misassignment in fuel CO_2 of about $0.8 \pm 0.8 \text{ } \mu\text{mol/mol}$ (\approx
3 5%). If there are nuclear power plants or fuel reprocessing plants in the catchment area of the
4 measurement site and if monthly mean emission data of pure $^{14}\text{C}(\text{CO}_2)$ from these nuclear facilities
5 are available, it is advisable to correct for them at the highest possible temporal resolution e.g.
6 using transport models (Vogel et al., 2013b). Note, that for the calibration of \overline{R}_F , $\overline{\delta}_F$, $\overline{\delta}_{ff}$ or $\overline{\delta}_{F-tr}$
7 using $\Delta^{14}\text{C}(\text{CO}_2)$ grab samples, it should be possible to choose the calibration grab samples via
8 trajectory forecast such that no nuclear power plant influences are encountered in the grab samples.
9 However, this limits the footprint area that can be sampled and calibrated.

10 We have compared the diurnal cycle of the tracer-based fuel CO_2 estimates for Heidelberg and
11 found that the tracer configurations using CO , $\delta^{13}\text{C}(\text{CO}_2)$ and $\Delta^{14}\text{C}(\text{CO}_2)$ were able to reproduce
12 the diurnal cycle well and show a mean difference of better than $5 \pm 15 \text{ \%}$ and a root mean square
13 difference of 15% at the most. This seems surprising, since one might expect a diurnal pattern of
14 $\overline{\delta}_F$ and \overline{R}_F due to a varying share of emissions of different emission sectors in the footprint, leading
15 to a systematic deviation of the estimated from the real modelled diurnal cycle. However, since the
16 diurnal patterns are small (e.g. peak to peak difference of $\delta^{13}\text{C}(\text{CO}_2)$ ca. 2 ‰), the mean diurnal
17 variations are not significantly improved when using a diurnal correction of the mean isotopic
18 source signatures. One should keep in mind that natural CO contributions may also vary
19 systematically on a diurnal basis. Such a natural systematic variation was not included into the
20 model simulation, but will potentially introduce a diurnal bias into the continuous fuel CO_2 estimate
21 in a real setting. Therefore, it may be necessary to model or approximate natural CO in a real
22 setting. It may be possible to approximate the (sub-monthly) natural CO component using
23 formaldehyde (HCHO) measurements, since the production of CO from NMHC pass HCHO as
24 intermediate molecule (Atkinson, 2000). However, the high dry deposition rate of HCHO may
25 complicate the interpretation further. Since afternoon values are often used in inverse model studies
26 to derive fluxes it is important, that afternoon fuel CO_2 values can be estimated accurately. This
27 could be confirmed for $\delta^{13}\text{C}(\text{CO}_2)$ and CO in this study (see Fig. 8).

28
29 In order to better study the biospheric carbon fluxes on all relevant scales, it is important to improve
30 fuel CO_2 bottom-up inventories, so that fuel and biospheric CO_2 can be separated for independent

1 use in inverse model approaches. At present, emission inventories typically have uncertainties of
2 30-150 % at regional resolution (Wang et al., 2013). We could show in our study that some tracer-
3 based approaches such as CO and $\delta^{13}\text{C}(\text{CO}_2)$ -based methods lead to uncertainties of fuel CO₂ of
4 30% and accuracies of 10% (after calibration). However, for retrieving improved emission
5 estimates using inverse models, also the model transport errors need to be taken into account and
6 convoluted with the accuracy of fuel CO₂ estimates. At the moment, the model transport errors are
7 usually larger during night time (ca. 100%) than in the afternoon (ca. 40%) (besides at mountain
8 sites), which is why mainly afternoon values are used in model inversions (Gerbig et al., 2008).
9 Obviously, but unfortunately during the afternoon hours, the fuel CO₂ signal is very small
10 complicating the unbiased estimation of fuel CO₂ emissions using continuous tracers in inverse
11 transport models in these hours until better transport models and boundary layer height models
12 exist.

13
14
15 Acknowledgment: We thank Ute Karstens and Thomas Koch for valuable modelling lessons and
16 help with setting up the model. We are also grateful for valuable discussions on fossil fuel CO₂ in
17 Heidelberg with Felix R. Vogel and Samuel Hammer. We would also like to thank Jocelyn
18 Turnbull and one anonymous referee for their valuable feedback. This work has been funded by
19 the InGOS EU project (284274) and ICOS BMBF project (01LK1225A).

21 **References**

22 Ahmadov, R., Gerbig, C., Kretschmer, R., Koerner, S., Neininger, B., Dolman, A. J. and Sarrat,
23 C.: Mesoscale covariance of transport and CO₂ fluxes: Evidence from observations and simulations
24 using the WRF-VPRM coupled atmosphere-biosphere model, *J. Geophys. Res.*, 112, D22107,
25 doi:10.1029/2007JD008552, 2007.

26
27 Atkinson, R.: Atmospheric chemistry of VOCs and NO_x, *Atmos. Environ.*, 34, 2063–2101, 2000.

28

1 Ballantyne, A. P., Miller, J. B., Baker, I. T., Tans, P. P., and White, J. W. C.: Novel applications of
2 carbon isotopes in atmospheric CO₂: what can atmospheric measurements teach us about processes
3 in the biosphere?, *Biogeosciences*, 8, 3093-3106, doi:10.5194/bg-8-3093-2011, 2011.
4

5 Bousquet, P., Peylin, P., Ciais, P., Le Quéré, C., Friedlingstein, P., & Tans, P. P. : Regional changes
6 in carbon dioxide fluxes of land and oceans since 1980. *Science*, 290(5495), 1342-1346, 2000.
7

8 BP: The role of biofuels beyond 2020, Technical report issued Sept. 2013. Available at:
9 <http://www.bp.com/en/global/alternative-energy/our-businesses/biofuels.html>, (last access:
10 23.02.2015)
11

12 Conrad R.: Soil microorganisms as controllers of atmospheric trace gases (H₂, CO, CH₄, OCS,
13 N₂O, and NO). *Microbiol Rev* 60:609–640, 1996.
14

15 Coyle, W.: The future of biofuels. Economic Research Service, Washington, DC, 2007.
16

17 Denier van der Gon, H.D., Hendriks, C., Kuenen, J., Segers, A., Visschedijk, A.; Description of
18 current temporal emission patterns and sensitivity of predicted AQ for temporal emission patterns,
19 TNP Report, EU FP7 MACC deliverable report D_D-EMIS_1.3. Available at: [https://gmes-](https://gmes-atmosphere.eu/documents/deliverables/d-emis/MACC_TNO_del_1_3_v2.pdf)
20 [atmosphere.eu/documents/deliverables/d-emis/MACC_TNO_del_1_3_v2.pdf](https://gmes-atmosphere.eu/documents/deliverables/d-emis/MACC_TNO_del_1_3_v2.pdf), 2011.
21

22 Djuricin, S., Pataki, D. E. and Xu, X.: A comparison of tracer methods for quantifying CO₂ sources
23 in an urban region, *J. Geophys. Res.*, 115, D11303, doi:10.1029/2009JD012236, 2010.
24

25 Dörr, H., B. Kromer, I. Levin, K. O. Münnich, and H.-J. Volpp: CO₂ and radon 222 as tracers for
26 atmospheric transport, *J. Geophys. Res.*, 88(C2), 1309–1313, doi:[10.1029/JC088iC02p01309](https://doi.org/10.1029/JC088iC02p01309),
27 1983.
28

1 Druffel, E. M., & Suess, H. E.: On the radiocarbon record in banded corals: exchange parameters
2 and net transport of $^{14}\text{CO}_2$ between atmosphere and surface ocean. *Journal of Geophysical*
3 *Research: Oceans*, 88(C2), 1271-1280, 1983.

4
5 European Commission –Joint Research Centre /PBL Netherlands Environmental Assessment
6 Agency. The Emissions Database for Global Atmospheric Research (EDGAR) version 4.3.
7 <http://edgar.jrc.ec.europa.eu/>, 2015

8
9 Esler, M. B., Griffith, D. W. T., Wilson, S. R., and Steele, L. P.: "Precision trace gas analysis by
10 FT-IR spectroscopy. 2. The $^{13}\text{C}/^{12}\text{C}$ isotope ratio of CO_2 ." *Analytical chemistry* 72.1 (2000): 216-
11 221.

12
13 Flanagan, L. B., Ehleringer, J. R., and Pataki D. E. (Eds.): *Stable isotopes and biosphere-*
14 *atmosphere interactions*, Elsevier Academic Press, San Diego, US, 318 pp., 2005.

15
16 Galli, I., Bartalini, S., Cancio, P., De Natale, P., Mazzotti, D., Giusfredi, G., Fedi, M.E. and
17 Mando, P. A.: Optical detection of radiocarbon dioxide: first results and AMS intercomparison.
18 *Radiocarbon*, 55(2-3), 213-223, 2013.

19
20
21 Gamnitzer, U., Karstens, U., Kromer, B., Neubert, R. E., Meijer, H. A., Schroeder, H., and Levin,
22 I.: Carbon monoxide: A quantitative tracer for fossil fuel CO_2 ?. *J. Geophys. Res. [Atmos.]* 111,
23 2006.

24
25 Gerbig, C., Lin, J. C., Wofsy, S. C., Daube, B. C., Andrews, A. E., Stephens, B. B., Bakwin, P. S.
26 and Grainger, C. A.: Toward constraining regional-scale fluxes of CO_2 with atmospheric
27 observations over a continent: 2. Analysis of COBRA data using a receptor-oriented framework, *J*
28 *Geophys Res-Atmos*, 108(D24), doi:10.1029/2003JD003770, 2003.

29
30

1 Gerbig, C., Körner, S. and Lin, J. C.: Vertical mixing in atmospheric tracer transport models: error
2 characterization and propagation, *Atmos. Chem. Phys.*, 8, 591–602, 2008.

3

4 Granier, C., Pétron, G., Müller, J.-F. and Brasseur, G. : The impact of natural and anthropogenic
5 hydrocarbons on the tropospheric budget of carbon monoxide. *Atmos. Environ.* 34, 5255–5270,
6 2000.

7

8 Graven, H. D., and Gruber, N.: Continental-scale enrichment of atmospheric $^{14}\text{CO}_2$ from the
9 nuclear power industry: potential impact on the estimation of fossil fuel-derived CO_2 . *Atmos.*
10 *Chem. Phys.* 11, 12339-12349, 2011.

11

12 Gros, V., Tsigaridis, K., Bonsang, B., Kanakidou, M., Pio, C.: Factors controlling the diurnal
13 variation of CO above a forested area in southeast Europe, *Atmos. Environ.* 36, 19, 3127-3135,
14 ISSN 1352-2310, 2002.

15

16 Gurney, K. R., Law, R. M., Denning, A. S., Rayner, P. J., Baker, D., Bousquet, P., Bruhwiler L.,
17 Chen, Y., Ciais, C., Fan, S., Fung, I. Y., Gloor, M., Heimann, M., Higuchi, John, J., Maki, T.,
18 Maksyutov, S., Masarie, K., Peylin, P., Prather, M., P, B.C., Randerson, J., Sarmiento, J., Taguc,
19 S., Takahashi, T., & Yuen, C. W. :Towards robust regional estimates of CO_2 sources and sinks
20 using atmospheric transport models. *Nature*, 415(6872), 626-630, 2002.

21

22 Gurney, K. R., Y.-H. Chen, T. Maki, S. R. Kawa, A. Andrews, and Z. Zhu: Sensitivity of
23 atmospheric CO_2 inversions to seasonal and interannual variations in fossil fuel emissions, *J.*
24 *Geophys. Res.*, 110, D10308, doi:10.1029/2004JD005373, 2005.

25

26 Hammer, S., Griffith, D. W. T., Konrad, G., Vardag, S., Caldow, C., and Levin, I.: Assessment of
27 a multi-species in situ FTIR for precise atmospheric greenhouse gas observations, *Atmos. Meas.*
28 *Tech.*, 6, 1153-1170, doi:10.5194/amt-6-1153-2013, 2013.

29

1 Heimann, M., and Koerner, S.: The global atmospheric tracer model TM3, Technical Reports,
2 Max-Planck-Institute for Biogeochemie, 5, 131 pp., 2003.

3

4 IEA, International Energy Agency: Key World Energy Statistics 2014, 2014, available at:
5 [http://www.iea.org/publications/freepublications/publication/key-world-energy-statistics-](http://www.iea.org/publications/freepublications/publication/key-world-energy-statistics-2014.html)
6 [2014.html](http://www.iea.org/publications/freepublications/publication/key-world-energy-statistics-2014.html) (last access: 30 Sept. 2015).

7

8 Inman, R. E., Ingersoll, R. B., Levy, E. A. : Soil: A natural sink for carbon monoxide, Science,
9 172(3989), 1229–1231, doi:10.1126/science.172.3989.1229, 1971.

10

11 Jung, M., Henkel, K., Herold, M., and Churkina, G.: Exploiting synergies of global land cover
12 products for carbon cycle modeling, Remote Sens. Environ., 101, 534–553, 2006.

13

14 Kaul, M.: Isotopenverhältnisse im atmosphärischem Kohlendioxid und seine Quellen im Raum
15 Heidelberg, Staatsexamensarbeit, 2007.

16

17 Keeling, C. D., The concentration and isotopic abundances of atmospheric carbon dioxide in rural
18 areas, Geochim Cosmochim Acta, 13, 322– 334, 1958.

19

20 Keeling, C. D., The concentration and isotopic abundance of carbon dioxide in rural and marine
21 air, Geochim. Cosmochim. Acta, 24, 277– 298, 1961.

22

23 Keeling, R. F., Piper, S.C. and Heimann, M.: Global and hemispheric CO₂ sinks deduced from
24 changes in atmospheric O₂ concentration, Nature 381, 218-221, 1996.

25

26 Le Quéré, C., Moriarty, R., Andrew, R. M., Peters, G. P., Ciais, P., Friedlingstein, P., Jones, S. D.,
27 Sitch, S., Tans, P., Arneeth, A., Boden, T. A., Bopp, L., Bozec, Y., Canadell, J. G., Chini, L. P.,
28 Chevallier, F., Cosca, C. E., Harris, I., Hoppema, M., Houghton, R. A., House, J. I., Jain, A. K.,
29 Johannessen, T., Kato, E., Keeling, R. F., Kitidis, V., Klein Goldewijk, K., Koven, C.,
30 Landa, C. S., Landschützer, P., Lenton, A., Lima, I. D., Marland, G., Mathis, J. T., Metzl, N.,

1 Nojiri, Y., Olsen, A., Ono, T., Peng, S., Peters, W., Pfeil, B., Poulter, B., Raupach, M. R.,
2 Regnier, P., Rödenbeck, C., Saito, S., Salisbury, J. E., Schuster, U., Schwinger, J., Séférian, R.,
3 Segschneider, J., Steinhoff, T., Stocker, B. D., Sutton, A. J., Takahashi, T., Tilbrook, B.,
4 van der Werf, G. R., Viovy, N., Wang, Y.-P., Wanninkhof, R., Wiltshire, A., and Zeng, N.: Global
5 carbon budget 2014, *Earth Syst. Sci. Data*, 7, 47-85, doi:10.5194/essd-7-47-2015, 2015.

6
7

8 Levin, I., Kromer, B., Schmidt, M., and Sartorius, H.: A novel approach for independent budgeting
9 of fossil fuel CO₂ over Europe by ¹⁴CO₂ observations, *Geophys. Res. Lett.*, 30(23), 2194,
10 doi:10.1029/2003GL018477, 2003.

11

12 Levin, I. and Karstens, U.: Inferring high-resolution fossil fuel CO₂ records at continental sites
13 from combined (CO₂)-C-14 and CO observations, *Tellus B*, 59, 245–250, doi:10.1111/j.1600-
14 0889.2006.00244.x, 2007.

15

16 Levin, I., Hammer, S., Kromer, B., Meinhardt, F.: Radiocarbon observations in atmospheric CO₂:
17 Determining fossil fuel CO₂ over Europe using Jungfraujoch observations as background, *Sci.*
18 *Total Environ.* 391, 211-216, ISSN 0048-9697, 2008.

19

20 Levin, I., Naegler, T., Kromer, B., Diehl, M., Francey, R. J., Gomez-Pelaez, A. J., Steele, L.P.,
21 Wagenbach, D., Weller, R. and Worthy, D. E.: Observations and modelling of the global
22 distribution and long-term trend of atmospheric ¹⁴CO₂. *Tellus B*, 62(1), 26-46, 2010.

23

24

25 Levin, I., Kromer, B., Hammer, S.: Atmospheric $\Delta^{14}\text{CO}_2$ trend in Western European background
26 air from 2000 to 2012, *Tellus B*, 2013.

27

28 Lin, J. C., C. Gerbig, S. C. Wofsy, A. E. Andrews, B. C. Daube, K. J. Davis, and C. A. Grainger
29 (2003), A near-field tool for simulating the upstream influence of atmospheric observations: The

1 Stochastic Time-Inverted Lagrangian Transport (STILT) model, *J. Geophys. Res.*, 108, 4493,
2 doi:10.1029/2002JD003161, D16.

3

4 Mahadevan, P., Wofsy, S. C., Matross, D. M., Xiao, X., Dunn, A. L., Lin, J. C., Gerbig, C., Munger,
5 J. W., Chow, V. Y., and Gottlieb, E. W.: A satellite-based biosphere parameterization for net
6 ecosystem CO₂ exchange: Vegetation Photosynthesis and Respiration Model (VPRM), *Global*
7 *Biogeochem. Cycles*, 22, doi:[10.1029/2006GB002735](https://doi.org/10.1029/2006GB002735), 2008.

8

9 Marland, G., Brenkert, A. and Olivier, J. (1999) CO₂ from fossil fuel burning: a comparison of
10 ORNL and EDGAR estimates of national emissions. *Environmental Science & Policy* 2, 265-273,
11 doi:10.1016/s1462-9011(99)00018-0.

12

13 McIntyre, C. P., McNicholm, A. P., Roberts, M.L., Seewald, J.S., von Reden, K.F., and Jenkins,
14 W.J.: Improved Precision of ¹⁴C Measurements for CH₄ and CO₂ Using GC and Continuous-Flow
15 AMS Achieved by Summation of Repeated Injections. *Radiocarbon*, 55, 2013.

16

17 Meijer, H. A. J., Smid, H. M. , Perez, E. Keizer, M. G.: Isotopic characterization of anthropogenic
18 CO₂ emissions using isotopic and radiocarbon analysis, *Phys. Chem. Earth*, 21(5–6), 483–487,
19 1996.

20

21 Miller, J. B., Lehman, S. J., Montzka, S. A., Sweeney, C., Miller, B. R., Karion, A., Wolak, C.,
22 Dlugokencky, E.J., Southon, J., Turnbull, J. C and Tans, P. P.: Linking emissions of fossil fuel CO₂
23 and other anthropogenic trace gases using atmospheric ¹⁴CO₂, *J. Geophys. Res.*, 117, D08302,
24 doi:10.1029/2011JD017048, 2012.

25

26 Mook, W. M. E. 2001. *Environmental Isotopes in the Hydrological Cycle. Principles and*
27 *Applications.* UNESCO/IAEA Series,
28 http://www.naweb.iaea.org/napc/ih/IHS_resources_publication_hydroCycle_en.html

1

2 Newman, S., Jeong, S., Fischer, M. L., Xu, X., Haman, C. L., Lefer, B., Alvarez, S.,
3 Rappenglueck, B., Kort, E. A., Andrews, A. E., Peischl, J., Gurney, K. R., Miller, C. E., and
4 Yung, Y. L.: Diurnal tracking of anthropogenic CO₂ emissions in the Los Angeles basin megacity
5 during spring 2010, *Atmos. Chem. Phys.*, 13, 4359-4372, doi:10.5194/acp-13-4359-2013, 2013.

6

7 Newman, S., Xu, X., Gurney, K. R., Hsu, Y.-K., Li, K.-F., Jiang, X., Keeling, R., Feng, S.,
8 O'Keefe, D., Patarasuk, R., Wong, K. W., Rao, P., Fischer, M. L., and Yung, Y. L.: Toward
9 consistency between bottom-up CO₂ emissions trends and top-down atmospheric measurements in
10 the Los Angeles megacity, *Atmos. Chem. Phys. Discuss.*, 15, 29591-29638, doi:10.5194/acpd-15-
11 29591-2015, 2015.

12

13 Nydal, R., Lövseth, K. and Gullicksen, S.: A survey of radiocarbon variation in nature since the
14 test ban treaty. University of California Press, Berkley, California, 1979.

15

16 Parrish, D. D., Trainer, M., Holloway, J.S., Yee, J., Warshawsky, S., Fehsenfeld, F., Forbes, G.,
17 Moody, J.: Relationships between ozone and carbon monoxide at surface sites in the North Atlantic
18 region, *J. Geophys. Res.*, 103(D11), 13,357–13,376, doi:10.1029/98JD00376, 1993.

19

20 Pataki, D. E., Ehleringer, J. R., Flanagan, L. B., Yakir, D., Bowling, D. R., Still, C. J., Buchmann,
21 N., Kaplan, J. O. and Berry, J. A.: The application and interpretation of Keeling plots in terrestrial
22 carbon cycle research, *Global Biogeochem. Cycles*, 17, 1022, doi:10.1029/2001GB001850, 1,
23 2003.

24

25 Pataki, D. E., Alig, R. J., Fung, A. S., Golubiewski, N. E., Kennedy, C. A., McPherson, E. G.,
26 Nowak, D. J., Pouyat, R. V., and Romero Lankao, P.: Urban ecosystems and the North American
27 carbon cycle, *Global Change Biol.*, 12, 2092–2102, doi:10.1111/j.1365-2486.2006.01242.x, 2006.

28

1 Peylin, P., Houweling, S., Krol, M. C., Karstens, U., Rödenbeck, C., Geels, C., Vermeulen, A.,
2 Badawy, B., Aulagnier, C., Pregger, T., Delage, F., Pieterse, G., Ciais, P., and Heimann, M.:
3 Importance of fossil fuel emission uncertainties over Europe for CO₂ modeling: model
4 intercomparison, *Atmos. Chem. Phys.*, 11, 6607-6622, doi:10.5194/acp-11-6607-2011, 2011.

5

6 Peylin, P., Law, R. M., Gurney, K. R., Chevallier, F., Jacobson, A. R., Maki, T., Niwa, Y., Patra,
7 P. K., Peters, W., Rayner, P. J., Rödenbeck, C., van der Laan-Luijkx, I. T., and Zhang, X.:
8 Global atmospheric carbon budget: results from an ensemble of atmospheric CO₂ inversions,
9 *Biogeosciences*, 10, 6699–6720, doi:10.5194/bg-10-6699-2013, 2013. 8885, 8887, 2013.

10

11 Prather, M., Ehhalt, D., Dentener, F., Derwent, R. G., Dlugokencky, E., Holland, E., Isaksen, I. S.
12 A., Katima, J., Kirchhoff, V., Matson, P., Midgley, P. M., and Wang, M.: Atmospheric chemistry
13 and greenhouse gases, in: *Climate Change 2001*, edited by: Houghton, J. T., 239–287, Cambridge
14 Univ. Press, New York, 2001.

15

16 Rödenbeck, C.: Estimating CO₂ sources and sinks from atmospheric mixing ratio measurements
17 using a global inversion of atmospheric transport, Max Planck Institute for Biogeochemistry, Jena,
18 Germany. [online] Available from: [http://www.bgc-jena.mpg.de/bgc-](http://www.bgc-jena.mpg.de/bgc-systems/pmwiki2/uploads/Publications/6.pdf)
19 [systems/pmwiki2/uploads/Publications/6.pdf](http://www.bgc-jena.mpg.de/bgc-systems/pmwiki2/uploads/Publications/6.pdf), 2005.

20

21 Rogelj, J., McCollum, D., Smith, S., Calvin, K., Clarke, L., Garg, A., Jiang, K., Krey, V., Lowe,
22 J., Riahi, K., Schaeffer, M., van Vuuren, D., Wenyang, C., Crippa, M., Janssens-Maenhout, G.,
23 Chapter 2 of The emission gap report 2014: What emission levels will comply with temperature
24 limit. In: *The emission gap report 2014: a UNEP synthesis report*. United Nations Environment
25 Programme (UNEP); 2014

26

27 Rivier, L., Ciais, P., Hauglustaine, D. A., Bakwin, P., Bousquet, P., Peylin, P., & Klonecki, A.:
28 Evaluation of SF₆, C₂Cl₄ and CO to approximate fossil fuel CO₂ in the Northern Hemisphere using
29 a chemistry transport model. *J. Geophys. Res.* 111, D16311, doi:10.1029/2005JD006725, 2006.

1

2 Schmidt, A., Rella, C. W., Göckede, M., Hanson, C., Yang, Z., Law, B.E.: Removing traffic
3 emissions from CO₂ time series measured at a tall tower using mobile measurements and transport
4 modeling, *Atmospheric Environment*, Volume 97, Pages 94-108, ISSN 1352-2310,
5 <http://dx.doi.org/10.1016/j.atmosenv.2014.08.006>, 2014.

6

7 Steinbach, J., Gerbig, C., Rödenbeck, C., Karstens, U., Minejima, C. and Mukai, H.: The CO₂
8 release and Oxygen uptake from Fossil Fuel Emission Estimate (COFFEE) dataset: effects from
9 varying oxidative ratios, *Atmos. Chem. Phys.*, 11(14), 6855–6870, doi:10.5194/acp-11-6855-2011,
10 2011.

11

12 Stohl, A., Forster, C., Frank, A., Seibert, P., Wotawa, G.: Technical note: the Lagrangian particle
13 dispersion model FLEXPART version 6.2. *Atmos Chem Phys* 5:2461–2474, 2005.

14

15 Stuiver, M., and Polach H.A.: Reporting of C-14 data-Discussion. *Radiocarbon* 19, 355-363, 1977.

16

17 Stuiver, M., and Quay, P. D.: Atmospheric ¹⁴C changes resulting from fossil fuel CO₂ release and
18 cosmic ray flux variability. *Earth and Planet. Sci. Lett.* 53, 349-362, 1981.

19

20 Suess, H. E: Radiocarbon concentration in modern wood. *Science* 122, 415-417, 1955.

21 Taylor, A. J., Lai, C. T., Hopkins, F. M., Wharton, S., Bible, K., Xu, X., Philipps, C., Bush.S. and
22 Ehleringer, J. R.: Radiocarbon-Based Partitioning of Soil Respiration in an Old-Growth Coniferous
23 Forest. *Ecosystems*, 1-12, 2015.

24

25 Trusilova, K., Roedenbeck, C., Gerbig, C. and Heimann, M.: Technical Note: A new coupled
26 system for global-to-regional downscaling of CO₂ concentration estimation, *Atmos. Chem. Phys.*,
27 10(7), 3205–3213, 2010.

1
2 Turnbull, J. C., Miller, J. B., Lehman, S. J., Tans, P. P., Sparks, R. J. and Southon, J.: Comparison
3 of $^{14}\text{CO}_2$, CO, and SF_6 as tracers for recently added fossil fuel CO_2 in the atmosphere and
4 implications for biological CO_2 exchange. *Geophys. Res. Lett.*, **33**, L01817, doi:
5 10.1029/2005GL024213, 2006.
6
7 Turnbull, J. C., S. J. Lehman, J. B. Miller, R. J. Sparks, J. R. Southon, and P. P. Tans : A new
8 high precision $^{14}\text{CO}_2$ time series for North American continental air, *J. Geophys. Res.*, 112,
9 D11310, doi:10.1029/2006JD008184, 2007.
10
11
12 Turnbull, J.C., Karion, A., Fischer, M.L., Faloona, I., Guilderson, T., Lehman, S.J., Miller, B.R.,
13 Miller, J.B., Montzka, S., Sherwood, T., Saripalli, S., Sweeney, C., Tans, P.P.: Assessment of
14 fossil fuel carbon dioxide and other anthropogenic trace gas emissions from airborne measurements
15 over Sacramento, California in spring 2009. *Atmos. Chem. Phys.* 11, 705-721, 2011.
16
17 Turnbull, J. C., Sweeney, C., Karion, A., Newberger, T., Lehman, S. J., Tans, P. P., Davis, K. J.,
18 Lauvaux, T., Miles, N. L., Richardson, S. J., Cambaliza, M. O., Shepson, P. B., Gurney, K.,
19 Patarasuk, R. Razlivanov, I.: Toward quantification and source sector identification of fossil fuel
20 CO_2 emissions from an urban area: Results from the INFLUX experiment. *Journal of Geophysical*
21 *Research: Atmospheres*, 2015.
22
23 Tuzson, B., Henne, S., Brunner, D., Steinbacher, M., Mohn, J., Buchmann, B., & Emmenegger, L.:
24 Continuous isotopic composition measurements of tropospheric CO_2 at Jungfrauoch (3580 m asl),
25 Switzerland: real-time observation of regional pollution events. *Atmos. Chem. Phys.*, 11(4), 1685-
26 1696, 2011.
27
28 Vardag, S. N., Hammer, S., O'Doherty, S., Spain, T. G., Wastine, B., Jordan, A., and Levin, I.:
29 Comparisons of continuous atmospheric CH_4 , CO_2 and N_2O measurements – results from a

1 travelling instrument campaign at Mace Head, Atmos. Chem. Phys., 14, 8403-8418,
2 doi:10.5194/acp-14-8403-2014, 2014.

3

4 Vogel, F. R.: $^{14}\text{CO}_2$ -calibrated carbon monoxide as proxy to estimate the regional fossil fuel CO_2
5 component at hourly resolution. PhD thesis, Ruprecht-Karls University Heidelberg, Germany,
6 2010.

7

8 Vogel, F., Hammer, S., Steinhof, A., Kromer, B., & Levin, I.: Implication of weekly and diurnal
9 ^{14}C calibration on hourly estimates of CO-based fossil fuel CO_2 at a moderately polluted site in
10 southwestern Germany. *Tellus B*, 62(5). doi: <http://dx.doi.org/10.3402/tellusb.v62i5.16600>, 2010.

11

12 Vogel, F. R., Huang, L., Ernst, D., Giroux, L., Racki, S., & Worthy, D. E. J.: Evaluation of a cavity
13 ring-down spectrometer for in situ observations of $^{13}\text{CO}_2$. *Atmospheric Measurement Techniques*,
14 6(2), 301-308, 2013a.

15

16 Vogel, F., Levin, I., Worthy, D.: Implications for Deriving Regional Fossil Fuel CO_2 Estimates
17 from Atmospheric Observations in a Hot Spot of Nuclear Power Plant $^{14}\text{CO}_2$ Emissions.
18 *Radiocarbon, North America*, 55, may. 2013b.

19

20 Wang, R., Tao, S., Ciais, P., Shen, H.Z., Huang, Y., Chen, H., Shen, G.F., Wang, B., Li, W.,
21 Zhang, Y. Y., Lu, Y., Zhu, D., Chen, Y.C., Liu, X.P., Wang, W.T., Wang, X.L., Liu, W.X. Li,
22 B.G., Piao, S.L.: High-resolution mapping of combustion processes and implications for CO_2
23 emissions, *Atmos. Chem. Phys.*, 13, pp. 1–15, 2013.

24

25 Widory, D., Proust, E., Bellenfant, G., Bour, O.: Assessing methane oxidation under landfill
26 covers and its contribution to the above atmospheric CO_2 levels: The added value of the isotope

1 ($\delta^{13}\text{C}$ and $\delta^{18}\text{O}$ CO_2 ; $\delta^{13}\text{C}$ and δD CH_4) approach, *Waste Manage*, 32, 9, 1685-1692, 0956-053X,
2 2012, Available at: <http://www.sciencedirect.com/science/article/pii/S0956053X12001729>.

3
4 Zondervan, A. and Meijer, H. A. J.: Isotopic characterisation of CO_2 sources during regional
5 pollution events using isotopic and radiocarbon analysis. *Tellus B*, 48: 601–612.
6 doi: 10.1034/j.1600-0889.1996.00013.x,1996.

7

8

9 **Appendix**

10 **A) Methods of continuous fuel CO_2 determination**

11 **A.1. Tracer configurations and their emission groups**

12 We formally introduce six different tracers or tracer combinations, which we use to estimate fuel
13 CO_2 continuously: CO_2 is used as sole tracer for fuel CO_2 . CO , $\delta^{13}\text{C}(\text{CO}_2)$ and $\Delta^{14}\text{C}(\text{CO}_2)$ records
14 are each used solely with CO_2 to estimate fuel CO_2 . Further, CO is used as tracer for traffic (and
15 $\delta^{13}\text{C}(\text{CO}_2)$ as tracer for fuel CO_2 minus traffic) and finally CO is used as tracer for biofuels (and
16 $\delta^{13}\text{C}(\text{CO}_2)$ as tracer for fuel CO_2 minus biofuels). The different emission groups are also listed and
17 characterized in Table A1.

18

19 *A.1.1. CO_2 as sole tracer for fuel CO_2*

20 When using CO_2 alone as “tracer” for fuel CO_2 ($y_F = y_{ff} + y_{bf}$), the total regional CO_2 offset is
21 assumed to solely originate from fuel emissions:

$$22 \quad y_F = \Delta y \quad (\text{A1})$$

23 With $\Delta y = y_{\text{tot}} - y_{\text{bg}}$.

24 This simple approach is valid, if (nearly) all CO_2 emissions are from fuel burning, as might be the
25 case in cold winters or in areas without biospheric activity (e.g. Mega cities).

1

2 *A.1.2. CO as tracer for fuel CO₂*

3 The CO offset ($\Delta x = x_{\text{tot}} - x_{\text{bg}}$) can be used to estimate fuel CO₂ offset if it is divided by the mean
4 ratio $\overline{R_F} = \Delta x / \Delta y_F$ of all fuel sources:

$$5 \quad y_F = \frac{\Delta x}{\overline{R_F}} \quad (\text{A2})$$

6 Note that in reality the ratio $\overline{R_F}$ varies, depending on the share of emissions of different emission
7 sectors in the catchment area, their temporal emission patterns, and due to natural CO sources and
8 sinks, at least in summer (Prather et al., 2001). We denote $\overline{R_F}$ with an overbar to emphasize that
9 this is a footprint-weighted average of the fuel emission ratio.

10

11 *A.1.3. CO as tracer for traffic CO₂ and $\delta^{13}\text{C}(\text{CO}_2)$ as tracer for all fuel CO₂, except for traffic CO₂*

12 We now include $\delta^{13}\text{C}(\text{CO}_2)$ in fuel CO₂ estimation as a tracer for all fuel CO₂ except those of
13 traffic ($y_{F-\text{tr}} = y_{\text{ff}} + y_{\text{bf}} - y_{\text{tr}}$).

$$14 \quad y_{\text{tot}} = y_{\text{bg}} + y_{\text{bio}} + y_{\text{tr}} + y_{F-\text{tr}} \quad (\text{A3})$$

$$15 \quad y_{\text{tot}} \delta_{\text{tot}} = y_{\text{bg}} \delta_{\text{bg}} + y_{\text{bio}} \delta_{\text{bio}} + y_{\text{tr}} \overline{\delta_{\text{tr}}} + y_{F-\text{tr}} \overline{\delta_{F-\text{tr}}} \quad (\text{A4})$$

16 In analogy to $\overline{R_F}$ we denote $\overline{\delta_{\text{tr}}}$ and $\overline{\delta_{F-\text{tr}}}$ with an overbar to emphasize that these are footprint-
17 weighted averages of the emission groups traffic CO₂ and fuel CO₂ excluding traffic, respectively.
18 Solving Eq. (A3) for y_{bio} , we can substitute y_{bio} in Eq. (A4). In analogy to Eq. (A2), we use CO as
19 tracer for traffic CO₂:

$$21 \quad y_{\text{tr}}(t) = \frac{x_{\text{tr}}(t)}{\overline{R_{\text{tr}}}} \quad (\text{A5})$$

20

22 With the mean $\Delta\text{CO}/\Delta\text{CO}_2$ ratio of traffic $\overline{R_{\text{tr}}} = (\Delta x / \Delta y)_{\text{tr}}$, CO_{tr} can be determined from:

$$23 \quad \text{CO}_{\text{tr}}(t) = \Delta\text{CO}(t) \cdot \overline{m_{\text{tr}}} \quad (\text{A6})$$

24 with $\overline{m_{\text{tr}}} = (\Delta x_{\text{tr}} / \Delta x)$ being the share of traffic CO to the total CO offset. $\overline{m_{\text{tr}}}$ needs to be estimated
25 from bottom-up inventories and can be found in Table A1 (right column) and is also dependent on

1 the footprint area of the measurement site and the sources and sinks lying in this area. Eq. (A3) –
 2 Eq. (A6) can then be re-arranged:

$$4 \quad y_{F-tr} = \frac{y_{tot}\delta_{tot} - y_{bg}\delta_{bg} - (y_{tot} - y_{bg} - y_{tr})\delta_{bio} - y_{2tr}\overline{\delta_{tr}}}{\overline{\delta_{F-tr}} - \delta_{bio}} \quad (A7)$$

5 Total fuel CO₂ (y_F) contribution can then be determined as the sum of y_{tr} (Eq. (A5)) and y_{F-tr} (Eq.
 6 (A7)).

7
 8 *A.1.4. CO as tracer for biofuel CO₂ and δ¹³C(CO₂) as tracer for all fuel CO₂, except for biofuel*
 9 *CO₂*

10 This method of fuel CO₂ estimation is in analogy to case A.1.3, but instead of separating fuel CO₂
 11 in to traffic contributions (y_{tr}) and others (y_{F-tr}), we separate it into biofuel contributions (y_{bf}) and
 12 others (y_{F-bf} = y_{ff}); this leads to:

$$14 \quad y_{F-bf} = \frac{y_{tot}\delta_{tot} - y_{bg}\delta_{bg} - (y_{tot} - y_{bg} - y_{bf})\delta_{bio} - y_{bf}\overline{\delta_{bf}}}{\overline{\delta_{ff}} - \delta_{bio}} \quad (A8)$$

15 Analogously to Eq. (A10), we formulate for y_{bf}:

$$17 \quad y_{bf}(t) = \frac{\Delta x(t) \cdot \overline{m_{bf}}}{R_{bf}} \quad (A9)$$

18 With $\overline{m_{bf}} = (\Delta x_{bf}/\Delta x)$ from bottom-up inventories (see Table A1). Total fuel CO₂ (y_F) is calculated
 19 as the sum of y_{bf} (Eq. (A9)) and y_{F-bf} (Eq. (A9)).

20
 21 *A.1.5. δ¹³C(CO₂) as sole tracer for fuel emission*

22 When using δ_{tot} as tracer for all fuel contributions, Eq. (A3) and Eq. (A4) simplify to

$$23 \quad y_F = \frac{y_{tot}\delta_{tot} - y_{bg}\delta_{bg} - (y_{tot} - y_{bg})\delta_{bio}}{\overline{\delta_F} - \delta_{bio}}$$

(A10)

if all fuel CO₂ (y_{F-tr} and y_{tr}) contributions are pooled to y_F .

A.1.6. $\Delta^{14}C(CO_2)$ as tracer for fossil fuel CO₂

Following Levin et al. (2008), we can derive fossil fuel CO₂ from $\Delta^{14}C(CO_2)$ and total CO₂ measurements according to:

$$y_{ff} = \frac{y_{bg} (\Delta^{14}C_{bg} - \Delta^{14}C_{bio}) - y_{tot} (\Delta^{14}C_{tot} - \Delta^{14}C_{bio}) - y_{bf} (\Delta^{14}C_{bio} - \Delta^{14}C_{bf})}{1 + \Delta^{14}C_{bio}}$$

(A11)

However, since $\Delta^{14}C_{bio} \approx \Delta^{14}C_{bf}$, and because biofuel contributions are not known, we neglect the last term of the numerator in the following. Note, that since $\Delta^{14}C(CO_2)$ is not sensitive to biofuel contributions, it is only possible to estimate the fossil fuel CO₂ contributions without biofuel contributions.

A.2 Determination of parameters and variables

The background values y_{bg} , x_{bg} , δ_{bg} and $\Delta^{14}C_{bg}$ should represent the regional clean air to which the source contributions from the footprint area are added. Since often, there are no nearby clean-air observations available for a polluted station, we use those mole fractions as background where the air masses in the boundary layer are well mixed with the free troposphere. This is usually the case in the afternoon and is associated with low mole fractions. Since CO₂, as well as CO both have local sinks relevant on the timescale of days, we here use CH₄ as an indicator for a well-mixed boundary layer and assume that, when the CH₄ mole fraction reaches a minimum value (within two days), vertical mixing is strongest. Principally, if continuous radon measurements were available, these could also be used as an indicator for vertical mixing (Dörr et al., 1983), instead of CH₄. We checked that the CH₄ minimum values always represent a lower envelope of the simulated greenhouse gas record and does not vary at the synoptic time scale. We then use the total mole fractions and isotopic records y_{tot} , x_{tot} , δ_{tot} , and $\Delta^{14}C_{tot}$ observed during situations with minimal CH₄ mole fractions as background values.

1 Further, in order to solve Eq. (A2)- Eq. (A11), we need the input parameters δ_{bio} , $\Delta^{14}\text{C}_{\text{bio}}$. These
2 input parameters were assigned with the objective to create realistic modelled data set (see Table
3 1 and A1). Additionally, the integrated footprint-weighted parameters $\overline{R_F}$, $\overline{R_{\text{tr}}}$, $\overline{R_{\text{bf}}}$, $\overline{\delta_F}$
4 $\overline{\delta_{\text{ff}}}$, $\overline{\delta_{\text{bf}}}$, $\overline{\delta_{\text{tr}}}$, $\overline{\delta_{\text{bio}}}$, $\overline{\delta_{\text{F-tr}}}$, $\overline{m_{\text{bf}}}$ and $\overline{m_{\text{tr}}}$ are required (see Table A1). We call these parameters
5 footprint-weighted, since the ratios and isotopic signatures depend on the relative contribution from
6 the different emission sectors (with their sector specific emission ratios and isotopic signatures)
7 within the footprint of the measurement site. We denote the integrated footprint-weighted
8 parameters with an overbar to draw attention to the fact that the parameters are averaged over the
9 (e.g. monthly) footprint area. Even though the emission factors of the source categories used here
10 are fixed for every pixel, integrated footprint-weighted $\overline{R_F}$, $\overline{R_{\text{tr}}}$, $\overline{R_{\text{bf}}}$, $\overline{\delta_F}$
11 $\overline{\delta_{\text{ff}}}$, $\overline{\delta_{\text{bf}}}$, $\overline{\delta_{\text{tr}}}$, $\overline{\delta_{\text{bio}}}$, $\overline{\delta_{\text{F-tr}}}$, $\overline{m_{\text{bf}}}$ and $\overline{m_{\text{tr}}}$ are not constant in time, because the footprint of the
12 measurement site and the emission patterns are temporally variable. Thus, the footprint-weighted
13 parameters change when the emissions from the different sectors or the footprint of the
14 measurement site vary. Note, that for our model study we do not require the parameters to be
15 absolutely correct, since we do not compare them to measured data. However, since we want to
16 provide a realistic case study, we seek to use the most realistic parameters (see values in Table 1
17 and A1).

18

19 **B) “Calibration” with $\Delta^{14}\text{C}(\text{CO}_2)$**

20 Solving Eq. (A3), (A8), (A9) and (A11) for fuel CO_2 requires $\overline{R_F}$, $\overline{\delta_F}$, $\overline{\delta_{\text{ff}}}$, and $\overline{\delta_{\text{F-tr}}}$. If these values
21 are not known, they may be derived from $\Delta^{14}\text{C}(\text{CO}_2)$ observations (what we then call $\Delta^{14}\text{C}(\text{CO}_2)$ -
22 calibrated). However, for the calibration y_{ff} must be known. The idea is to calibrate fossil fuel CO_2 ,
23 e.g. with precise $\Delta^{14}\text{C}(\text{CO}_2)$ measurements, on a lower time resolution (e.g. monthly) and assume
24 that the footprint-weighted parameters $\overline{R_F}$, $\overline{\delta_F}$, $\overline{\delta_{\text{ff}}}$, and $\overline{\delta_{\text{F-tr}}}$ do not change significantly within this
25 calibration interval.

26 Re-arranging Eq. (1) and (2) for $\overline{\delta_{\text{ff}}}$ and averaging it monthly leads to

$$28 \quad \overline{\delta_{\text{ff}}} = \frac{y_{\text{tot}}\delta_{\text{tot}} - y_{\text{bg}}\delta_{\text{bg}} - (y_{\text{tot}} - y_{\text{bg}} - y_{\text{ff}} - y_{\text{bf}})\delta_{\text{bio}} - y_{\text{bf}}\overline{\delta_{\text{bf}}}}{y_{\text{ff}}}$$

27

(B1)

1 , which could then be used in Eq. (A9). Note that we require the biofuel CO₂ in addition to the
 2 fossil fuel CO₂ from $\Delta^{14}\text{C}(\text{CO}_2)$.

3 $\overline{\delta_F}$ can then be derived, if the y_{bf} concentration is known.

$$5 \quad \overline{\delta_F} = \frac{\overline{\delta_{\text{ff}}} y_{\text{ff}} + \overline{\delta_{\text{bf}}} y_{\text{bf}}}{y_{\text{ff}} + y_{\text{bf}}}$$

4 (B2)

6 If fossil fuel emissions are divided into fossil fuel contributions without traffic ($y_{\text{F-tr}}$) and traffic
 7 contributions (y_{tr}), we can derive $\overline{\delta_{\text{F-tr}}}$ required for solving Eq (A8):

$$9 \quad \overline{\delta_{\text{F-tr}}} = \frac{\overline{\delta_{\text{F}}} y_{\text{F}} - \overline{\delta_{\text{tr}}} y_{\text{tr}}}{y_{\text{F}} - y_{\text{tr}}}$$

8 (B3)

10 Analogously, the ratio $\overline{R_F}$ could be calibrated following:

$$12 \quad \overline{R_F} = \frac{\Delta x}{\Delta y_F}$$

11 (B4)

13 In order to calculate the monthly mean value of $\langle \overline{\delta_F} \rangle$ and $\langle \overline{R_F} \rangle$, the mean ratios $\langle \frac{\Delta x}{\Delta y_F} \rangle$ (Eq. (B1)-
 14 (B4)) are needed. However, from integrated $\Delta^{14}\text{C}(\text{CO}_2)$ sampling, we only have the mean fossil
 15 fuel CO₂ and fuel CO₂ values and can thus, only calculate $\frac{\langle \Delta x \rangle}{\langle \Delta y_F \rangle}$. Using the product (or ratio) of the
 16 means rather than the mean of the product (ratio) is only correct if the factors are uncorrelated.
 17 Since, the factors in Eq. (B1) - (B4) (and Δx and Δy_{ff}) are correlated, the integrated calibration
 18 cannot be applied without introducing a bias into monthly mean $\langle \overline{\delta_F} \rangle$, $\langle \overline{\delta_{\text{ff}}} \rangle$, $\langle \overline{\delta_{\text{F-tr}}} \rangle$ and $\langle \overline{R_F} \rangle$. Instead
 19 of using integrated $\Delta^{14}\text{C}(\text{CO}_2)$ samples in order to obtain the monthly fossil fuel CO₂ values, it is
 20 possible to take grab samples, analyse these for $\Delta^{14}\text{C}(\text{CO}_2)$ (and with that y_{ff}), total CO₂,
 21 $\delta^{13}\text{C}(\text{CO}_2)_{\text{tot}}$ and CO in order to calculate the individual (non-averaged) values for $\overline{\delta_F}$, $\overline{\delta_{\text{F-tr}}}$, $\overline{\delta_{\text{ff}}}$ and
 22 $\overline{R_F}$ (see Sect. 4).

23

24 C) Influence of more depleted fuel $\delta^{13}\text{C}(\text{CO}_2)$ signatures

1 We have argued that we only require a realistic set of input parameters, rather than an absolutely
2 correct set of parameters to estimate uncertainties of the different tracer methods. However, the
3 results presented so far are to some degree dependent on the emission characteristics used in our
4 model (see Table A1). When using CO as tracer for fuel CO₂, it would be advantageous if natural
5 sources of CO were negligible and if the emission ratio \overline{R}_F would be the same for all sources. When
6 using CO₂ as tracer for fuel CO₂, biospheric CO₂ emissions should be negligible, and when using
7 $\delta^{13}\text{C}(\text{CO}_2)$, it would be advantageous if fuel CO₂ emissions were strongly depleted compared to
8 biospheric emissions. It is beyond the scope of this work, to show explicitly for all cases how the
9 “choice” of different emission characteristics influences the fuel CO₂ estimate in terms of precision
10 and accuracy. However, in Figure A1, we illustrate exemplary for this latter case how the presence
11 of more depleted fuel sources in the footprint area of the measurement site could improve the tracer
12 $\delta^{13}\text{C}(\text{CO}_2)$ for fuel CO₂ estimation. This should serve as an example, showing how much the
13 emission characteristics at a site may influence the precision of fuel CO₂ estimates using different
14 tracer configurations.

15
16 Figure A1 shows that fuel CO₂ can be estimated much better when the mean source mix in the
17 catchment area of the measurement site exhibits a strongly depleted isotopic source signature. The
18 regression coefficient improves from 0.94 to 0.99 and the precision within one year decreases
19 significantly by 40 % when choosing $\overline{\delta}_F$ 7 ‰ more depleted (-39 ‰ instead of -32 ‰). The
20 precision of $\delta^{13}\text{C}(\text{CO}_2)$ -based fuel CO₂ will increase with decreasing isotopic signature of fuel
21 CO₂ sources. Analogously, the precision of CO-based fuel CO₂ estimates will increase with
22 decreasing inhomogeneity of CO/CO₂ ratio of fuel CO₂ sources. This effect should be taken into
23 account when designing a measurement network and thus highlights the importance of a thorough
24 source evaluation in the catchment area prior to instrumental installation.

25
26
27
28
29

1
2
3
4
5
6
7
8
9
10
11
12
13
14
15
16
17
18
19
20
21
22
23

List of acronyms

- AMS - accelerator mass spectrometry
- bf – Biofuel
- bg – Background
- bio – Biosphere
- EDGAR- Emissions Database for Global Atmospheric Research
- F – Fuel
- F-bf – Fuel excluding biofuels (=ff)
- ff – Fossil fuel
- F-tr – Fuel excluding traffic
- GC - Gas chromatography
- ICOS – Integrated Carbon Observation System
- IQR- Inter-quartile range
- m_x – CO share of emission group x to CO offset
- NPP- Nuclear power plant
- ppm – parts per million, equivalent to μmol/mol

- 1 R_x – Ratio of CO to CO₂ in the emission group x
- 2 sd- Standard deviation
- 3 STILT – Stochastic Time-Inverted Lagrangian Particle model
- 4 tot – Total
- 5 x - CO mole fraction
- 6 y - CO₂ mole fraction

7

8 Table 1: $\delta^{13}\text{C}(\text{CO}_2)$ source signature of fuel types and biosphere as used in the model. The isotopic
 9 signature of the biosphere follows the findings of Ballantyne et al. (2011) for Europe. The assigned
 10 isotopic fuel values were chosen from mean measured isotopic signatures in Heidelberg (Kaul,
 11 2007 and unpublished data) or if not available, are similar to isotopic $\delta^{13}\text{C}(\text{CO}_2)$ values reported in
 12 Andres et al. (1994) or (for biogas) Widory et al. (2012).

| Emission source | $\delta_{\text{ff},i}$, $\delta_{\text{bf},j}$ or δ_{bio} |
|-----------------|--|
| | [‰] |
| Hard coal | -27 |
| Brown coal | -29 |
| Peat | -30 |
| Solid waste | -30 |
| Heavy oil | -31 |
| Light oil | -31 |
| Natural gas | -48 |
| Derived gas | -30 |
| Solid biomass | -29 |

| | |
|------------|-----|
| Bio liquid | -31 |
| Biosphere | |
| Jan | -27 |
| Feb | -26 |
| Mar | -25 |
| Apr | -24 |
| May | -23 |
| Jun | -22 |
| July | -22 |
| Aug | -23 |
| Sep | -24 |
| Oct | -25 |
| Nov | -26 |
| Dec | -27 |

1

2 Table 2: Tracer or tracer combinations, required parameters and formula for estimation of targeted
3 fuel CO₂ concentration. In cases c) and d) we further divide fuel CO₂ into traffic CO₂ and non-
4 traffic CO₂, or fossil fuel CO₂ and biofuel CO₂, respectively. In case f) we can only estimate fossil
5 fuel CO₂ with $\Delta^{14}\text{C}(\text{CO}_2)$ and therefore lack biofuel CO₂ for a comprehensive fuel CO₂ estimate.

| Case | Required parameters | Formula (for derivation see Appendix A1) |
|--------------------|--|--|
| a) CO ₂ | - | $y_F = \Delta y$ |
| b) CO | \overline{R}_F | $y_F = \frac{\Delta x}{\overline{R}_F}$ |
| c) CO(tr) | $\overline{R}_{tr}, \overline{m}_{tr}$ | $y_F = \frac{\Delta x(t) \cdot \overline{m}_{tr}}{\overline{R}_{tr}} + \frac{y_{tot} \delta_{tot} - y_{bg} \delta_{bg} - (y_{tot} - y_{bg} - y_{tr}) \delta_{bio} - y_{tr} \overline{\delta}_{tr}}{(\overline{\delta}_{F-tr} - \delta_{bio})} y_{tot}$ |

$$\begin{aligned}
& + \delta^{13}\text{C-CO}_2 & \overline{\delta_{tr}}, \overline{\delta_{F-tr}} \\
\text{d) CO(bf)} & \overline{R_{bf}}, \overline{m_{bf}}, & y_F = \frac{\Delta x(t) \cdot \overline{m_{bf}}}{\overline{R_{bf}}} + \frac{y_{tot}\delta_{tot} - y_{bg}\delta_{bg} - (y_{tot} - y_{bg} - y_{tr})\delta_{bio} - y_{bf}\overline{\delta_{bf}}}{(\overline{\delta_{ff}} - \delta_{bio})} y_{tot} \\
& + \delta^{13}\text{C-CO}_2 & \overline{\delta_{bf}}, \overline{\delta_{ff}} \\
\text{e) } \delta^{13}\text{C-CO}_2 & \overline{\delta_F} & y_F = \frac{y_{tot}\delta_{tot} - y_{bg}\delta_{bg} - (y_{tot} - y_{bg})\delta_{bio}}{(\overline{\delta_F} - \delta_{bio})} y_{tot} \\
\text{f) } \Delta^{14}\text{C-CO}_2 & \Delta^{14}\text{C}_{bf}, & y_F \approx y_{ff} = \frac{y_{bg}(\Delta^{14}\text{C}_{bg} - \Delta^{14}\text{C}_{bio}) - y_{tot}(\Delta^{14}\text{C}_{tot} - \Delta^{14}\text{C}_{bio}) - y_{bf}(\Delta^{14}\text{C}_{bio} - \Delta^{14}\text{C}_{bf})}{(\Delta^{14}\text{C}_{bio} + 1000)} \\
& \Delta^{14}\text{C}_{bio} &
\end{aligned}$$

1
2 Table 3: Magnitude, physical reason and reference of parameter variation, which are included in
3 Fig. 5-7

4

| Component | Variation (random) | Physical reason for variation | Reference |
|--|--------------------------|--|---|
| y_{tot}, y_{bg} | 0.05 $\mu\text{mol/mol}$ | Measurement uncertainty | Hammer et al., 2013 |
| $\delta_{meas}, \delta_{bg}$ | 0.05 % | Measurement uncertainty | e.g. Tuzson et al., 2011; Vardag et al., 2015 |
| x_{tot} | 15 nmol/mol | natural CO sources and sinks | Gros et al., 2002; Vogel, 2010 |
| δ_{bio} | 2 % | heterogeneity of biosphere | cmp. to Pataki et al., 2003 |
| $\Delta^{14}\text{C}_{meas}, \Delta^{14}\text{C}_{bg}$ | 5 % | Measurement uncertainty | McIntyre et al., 2013 |
| $\Delta^{14}\text{C}_{bio}$ | 5 % | heterogeneity of biosphere and turn-over times | cmp. Taylor et al., 2015 |
| $\Delta^{14}\text{C}_{bf}$ | 10 % | Source/Age of biofuels | -- |

| | | |
|---|---|-----------------------------------|
| $\overline{R_F}, \overline{R_{tr}}, \overline{R_{bf}}, \overline{\delta_F}$ $\overline{\delta_{ff}}, \overline{\delta_{bf}}, \overline{\delta_{tr}}, \overline{\delta_{F-tr}}, \overline{m_{bf}}$ and $\overline{m_{tr}}$ | -- Submonthly variation already included as only monthly median values are used, but parameters vary at an hourly time scale | Footprint or source mix change |
|---|---|-----------------------------------|

1

2

3

4

5

6 Table 4: Mean difference of tracer-based estimate and modelled (as correct assumed) fuel CO₂ in
7 μmol/mol for the tracers CO and δ¹³C(CO₂) for different sampling strategies and respective
8 standard deviation (both determined from a Gaussian fit to the difference histogram) for an urban
9 setting (here: Heidelberg). Depending on the random selection of grab samples, the bias of the
10 calibration with annually distributed grab samples is sometimes positive and sometimes negative.
11 Therefore, the mean absolute difference between the modelled and calibrated value was determined
12 in a Monte-Carlo simulation and is denoted with a “±” in front of the mean value to show that the
13 bias does not have a unique sign. The standard deviation denotes the 1-σ uncertainty of the
14 difference, which is always bi-directional. Note, that we only show the results for CO and
15 δ¹³C(CO₂), since the results when using a combination of these tracers is very similar to those of
16 the δ¹³C(CO₂)-method. Measurement uncertainties are included in all calibration methods.

| Method | CO mole fraction | | $\delta^{13}\text{C-CO}_2$ | |
|--|---------------------------|-------------------|----------------------------|-------------------|
| | Summer | Winter | Summer | Winter |
| No uncertainties, monthly median values known (as shown in Fig. 1) | 0.0 ± 2.1 | -0.3 ± 2.0 | 0.0 ± 0.7 | 0.1 ± 1.0 |
| Measurement uncertainties included, monthly median values known (as shown in Fig. 5) | -0.2 ± 4.3 | -0.3 ± 3.7 | -0.1 ± 3.5 | 0.0 ± 4.2 |
| Calibration with integrated samples (method 1) | n=24 -0.8 ± 4.9 | -0.7 ± 4.0 | -2.4 ± 5.2 | -1.8 ± 5.1 |
| Calibration with annually distributed grab samples (method 2) | n=24 $\pm 1.2 \pm 5.3$ | $\pm 1.5 \pm 4.7$ | $\pm 0.8 \pm 4.0$ | $\pm 1.6 \pm 4.9$ |
| | n=96 $\pm 1.1 \pm 5.2$ | $\pm 1.3 \pm 4.5$ | $\pm 0.5 \pm 3.8$ | $\pm 1.1 \pm 4.5$ |
| Calibration with seasonal grab sample calibration (method 3) | n=24 $\pm 1.2 \pm 5.3$ | $\pm 1.5 \pm 4.7$ | $\pm 1.6 \pm 4.6$ | $\pm 1.6 \pm 4.9$ |
| | n=96 $\pm 0.8 \pm 4.8$ | $\pm 1.1 \pm 4.3$ | $\pm 0.9 \pm 4.3$ | $\pm 0.8 \pm 4.3$ |
| Seasonal event calibration (method 4) | n=24 $\pm 2.1 \pm 6.1$ | $\pm 2.0 \pm 5.1$ | $\pm 1.2 \pm 4.3$ | $\pm 1.9 \pm 5.1$ |
| | n=96 $\pm 1.5 \pm 5.6$ | $\pm 1.9 \pm 4.9$ | $\pm 1.1 \pm 4.2$ | $\pm 1.3 \pm 4.6$ |

1

2

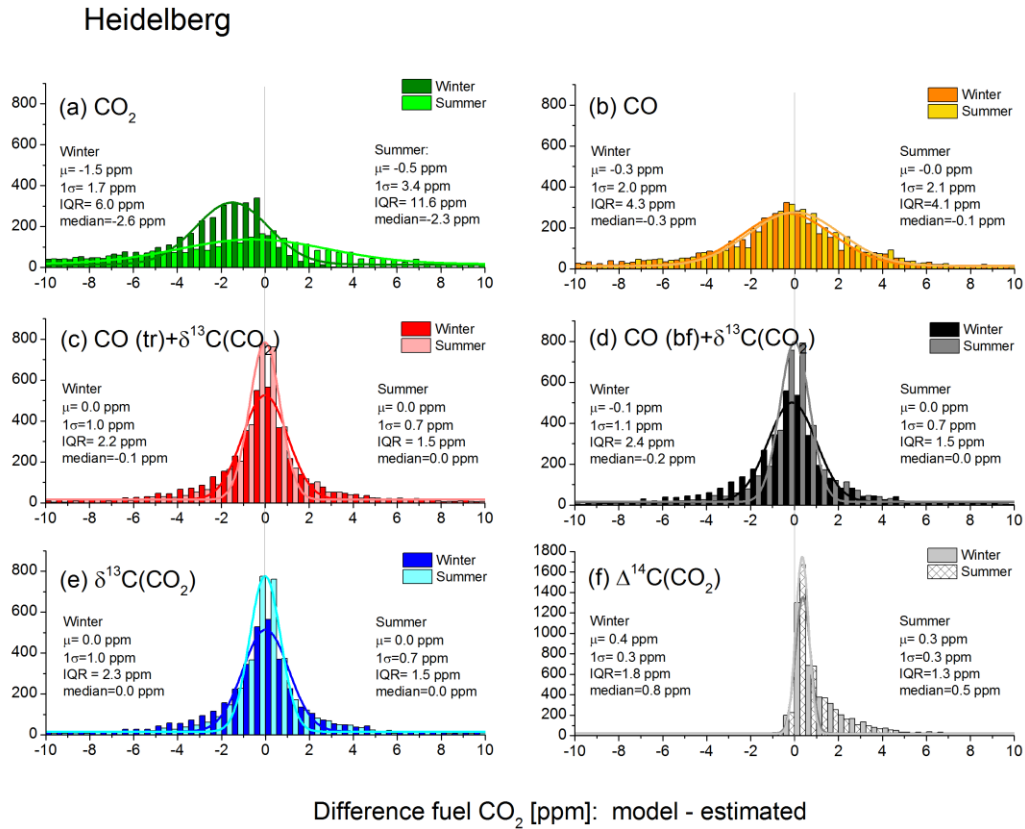
3

1 Table A1: Annual or half-yearly (summer = S, winter = W) averaged $\Delta^{14}\text{C}(\text{CO}_2)$, $\delta^{13}\text{C}(\text{CO}_2)$,
2 $\Delta\text{CO}/\Delta\text{CO}_2$ ratios and mean fraction of CO_2 and CO relative to total CO_2 and CO offsets as used
3 in our model study for the measurement site Heidelberg for the year 2012. Biosphere $\Delta^{14}\text{C}(\text{CO}_2)$
4 values are based on Taylor et al. (2015). The $\Delta\text{CO}/\Delta\text{CO}_2$ ratio and the fractions of CO_2 and CO
5 offset were taken from the STILT model runs, which were fed with anthropogenic emissions from
6 the EDGAR emission inventory. Note, that fractions of biofuels in traffic CO_2 emissions are not
7 included. δ values were derived by assigning an isotopic value to each fuel type and weighting
8 these depending on the respective share of the fuel type to total fuel CO_2 at the measurement site.
9 The δ -values of the biosphere are the half-yearly mean values from Table 1. Analogously, R_x (and
10 $\Delta^{14}\text{C}_x$) values were derived by assigning an emission ratio CO/CO_2 (and $\Delta^{14}\text{C}(\text{CO}_2)$ value) to each
11 emission sector and weighting these depending on the respective share of the emission sector to
12 total fuel CO_2 at the site.

13

| Emission group | $\Delta^{14}\text{C}-\text{CO}_2$ [‰] | $\delta^{13}\text{C}$ [‰] | | $\bar{R}_x =$ $(\Delta\text{CO}/\Delta\text{CO}_2)_x$ [ppb/ppm] | % of ΔCO_2 | | % of ΔCO | |
|---|--|---------------------------|-------|---|--------------------------|-----------|----------------------------|----------------------------|
| | | S | W | | S | W | S | W |
| Fuel CO_2 | -995 | -31.5 | -33.5 | 7 | 50 | 80 | 100 | 100 |
| Fossil fuel CO_2 (excl. biofuels) | -1000 | -32 | -34 | 3 | 45 | 70 | 50 | 37 |
| Biofuel CO_2 | 90 | -27 | -28 | 30 | 5 | 10 | \overline{m}_{bf} =50 | \overline{m}_{bf} =63 |
| Fuel CO_2 excl. traffic CO_2 (but incl. biofuels) | -990 | -31.5 | -33.8 | 7 | 35 | 67 | 70 | 80 |
| Traffic fuel CO_2 | -1000 | -31 | -31 | 7 | 15 | 13 | \overline{m}_{tr} =30 | \overline{m}_{tr} =20 |
| Biospheric CO_2 | 60 | -23 | -25.5 | 0 | 50 | 20 | 0 | 0 |

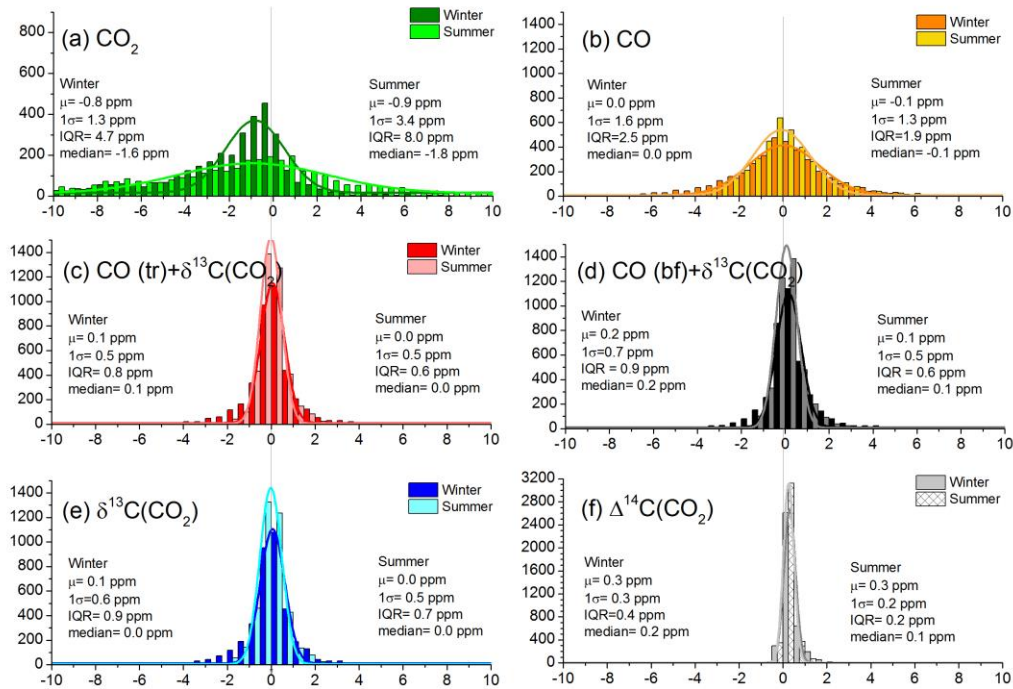
1



2

3 Figure 1: Histograms showing the differences between the modeled fuel CO_2 (assumed as correct)
4 and the tracer-based estimated fuel CO_2 for the year 2012 for Heidelberg using the different tracers
5 and tracer configurations listed in Table 2. Differences result from sub-monthly variations of
6 parameters. Note the different y-axis scale. Darker colors denote the winter periods and lighter
7 colors the summer periods (see legend). The distributions were fitted with a Gaussian fit and the
8 shift (μ) and the standard deviation (σ) for the Gaussian fits are given in the figure. Since the
9 histograms do not follow Gaussian distributions (especially for $^{14}\text{C}(\text{CO}_2)$ due to not normally
10 distributed biofuel CO_2 contributions within one year) we also give the Interquartile range (IQR)
11 in the figure to remind the reader that the uncertainty may be underestimated when using the
12 Gaussian standard deviation for uncertainty analysis. The CO_2 mole fractions are given in parts per
13 million (ppm), which is equivalent to $\mu\text{mol}/\text{mol}$. Note that in Heidelberg, mean fuel CO_2 for
14 summer is $15 \mu\text{mol}/\text{mol}$ and for winter is $16 \mu\text{mol}/\text{mol}$.

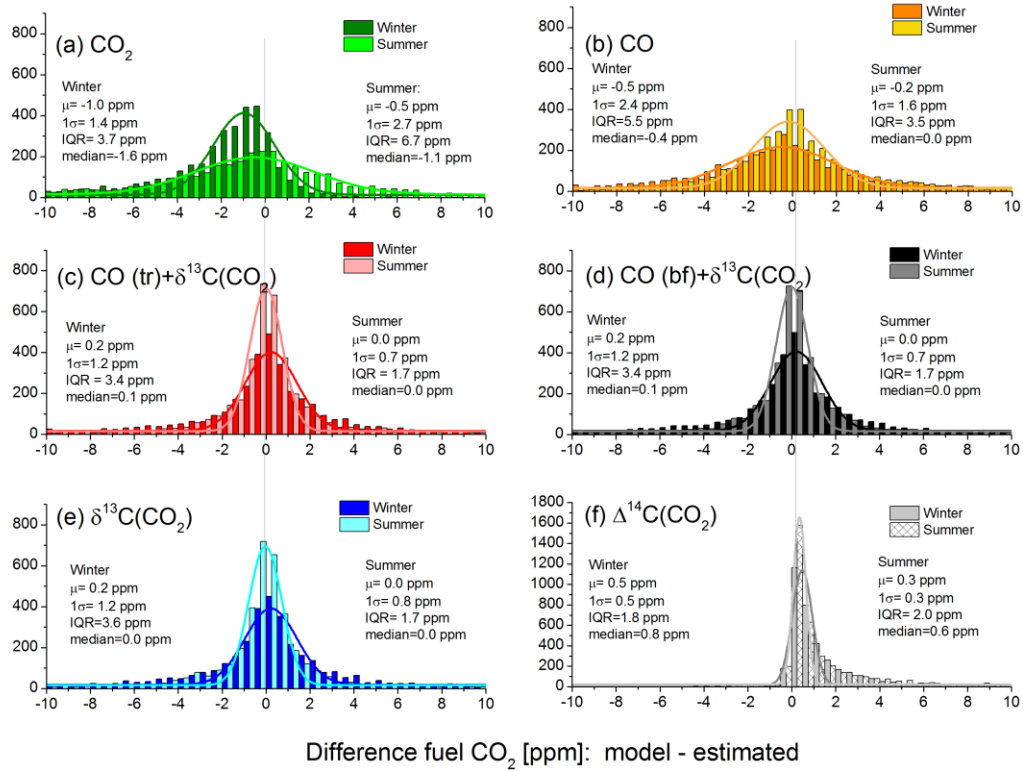
Gartow



Difference fuel CO_2 [ppm]: model - estimated

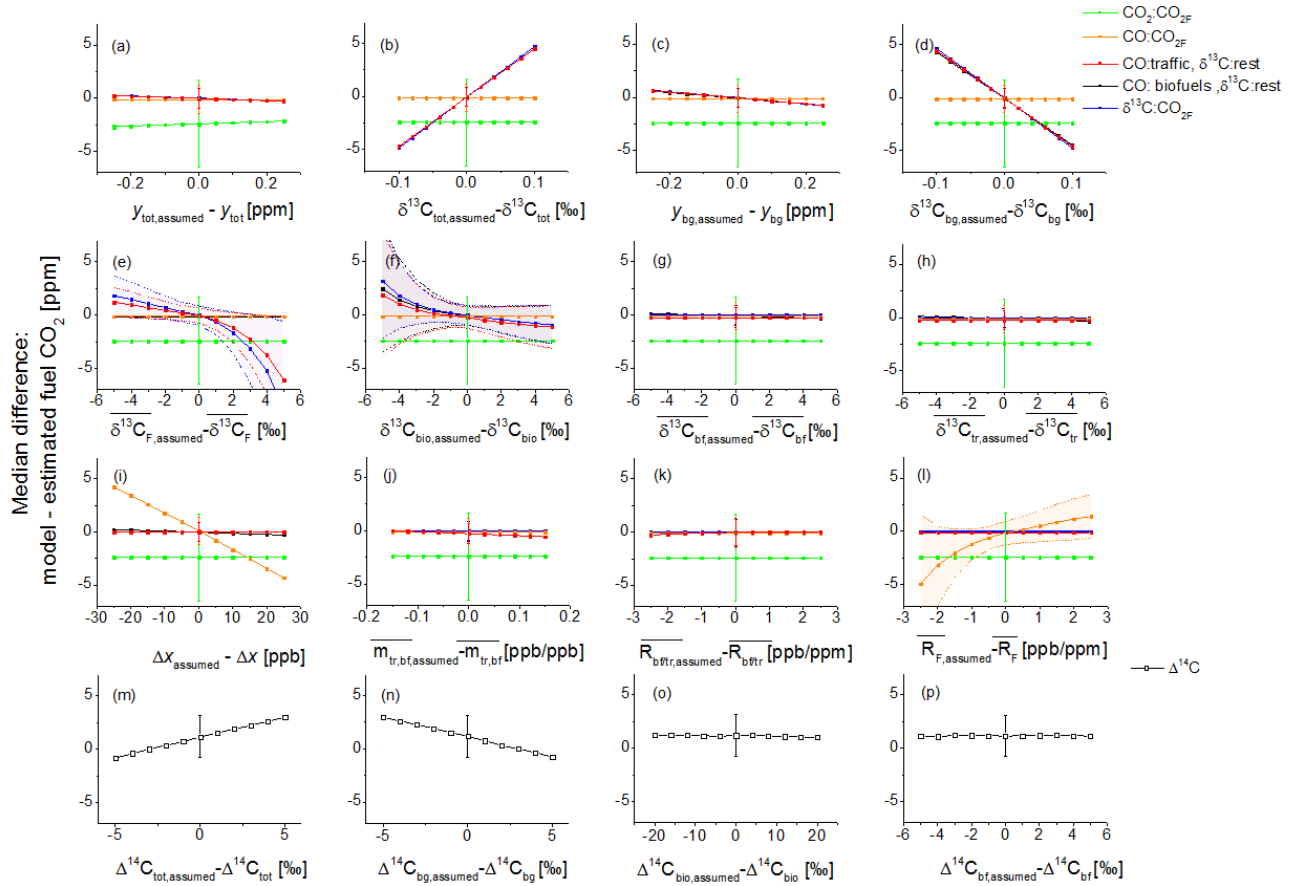
- 1
- 2 Figure 2: Same as Fig. 1, but for Gartow. In Gartow, mean fuel CO_2 for summer is 2 $\mu\text{mol/mol}$ and
- 3 for winter is 4 $\mu\text{mol/mol}$.

Berlin



- 1
- 2 Figure 3: Same as Fig. 1, but for Berlin. In Berlin, mean fuel CO_2 for summer is $23 \mu\text{mol/mol}$ and
- 3 for winter is $27 \mu\text{mol/mol}$.

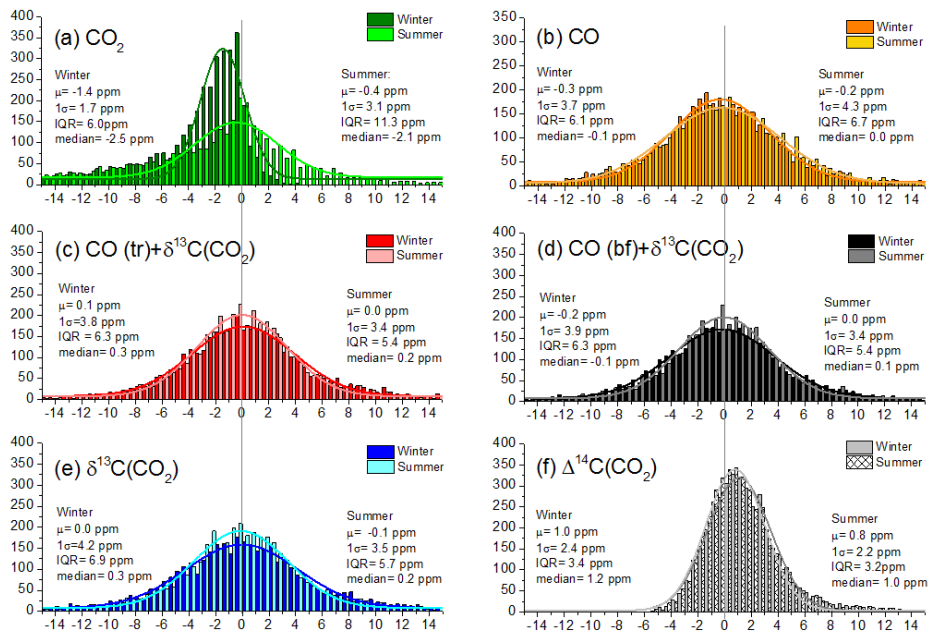
1



2

3 Figure 4: Sensitivity analysis: Median difference between the modelled fuel CO₂ and the tracer-
 4 based estimated fuel CO₂ value (y-axis) at a typical urban site (Heidelberg) when using
 5 parameters/variables for fuel CO₂ estimation (“assumed”) deviating from the correct
 6 parameters/variables used in STILT. The error bars given at x=0 (assumed value = model value)
 7 denote the Inter-quartile ranges (IQR) for all x-positions. If the IQRs vary depending on the
 8 assumed value, the errors (IQRs) are drawn as shaded areas.

Heidelberg - with measurement imprecision

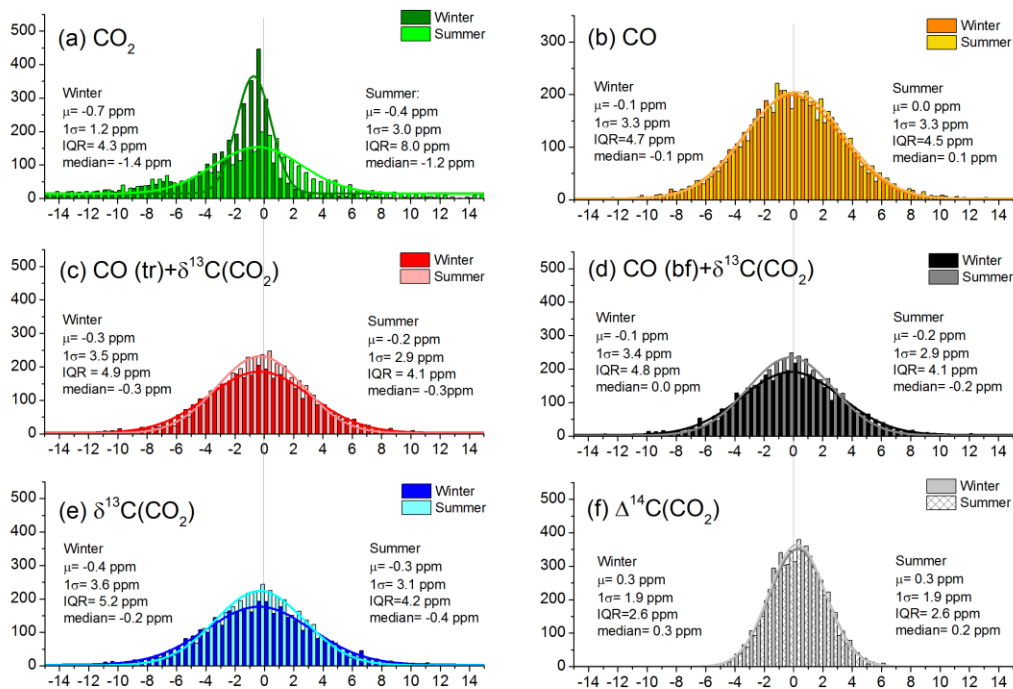


Difference fuel CO₂ [ppm]: model - estimated

1

2 Figure 5: Same as Fig. 1, but now also including measurement imprecision.

Gartow - with measurement imprecision

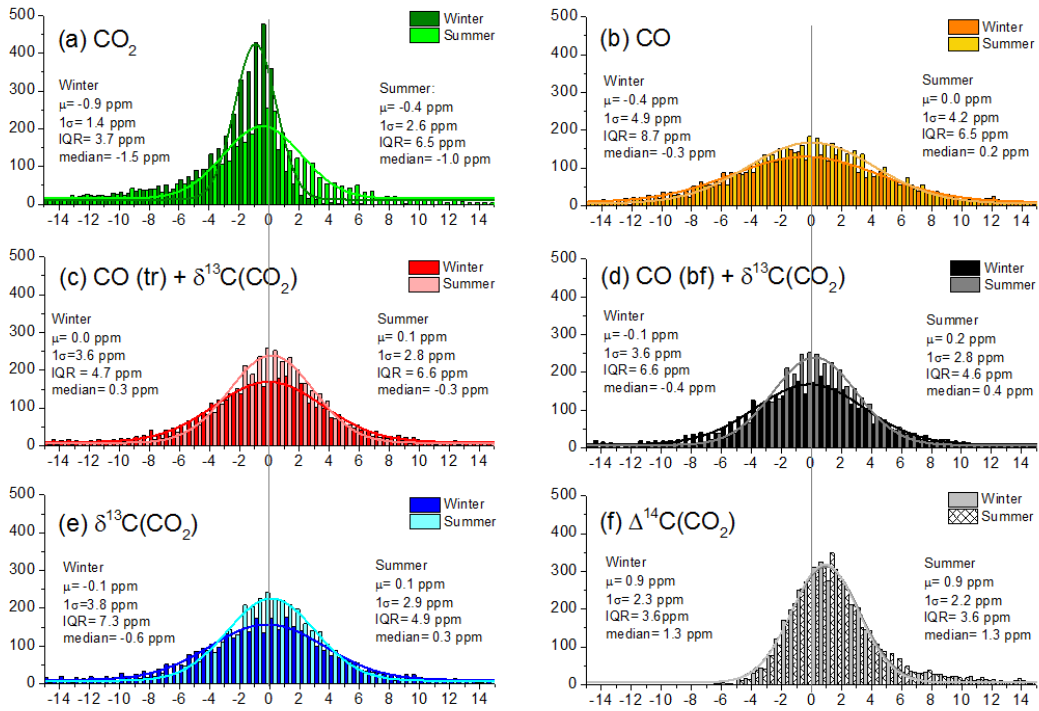


Difference fuel CO₂ [ppm]: model - estimated

1

2 Figure 6: Same as Fig. 2, but now also including measurement imprecision.

Berlin - with measurement imprecision

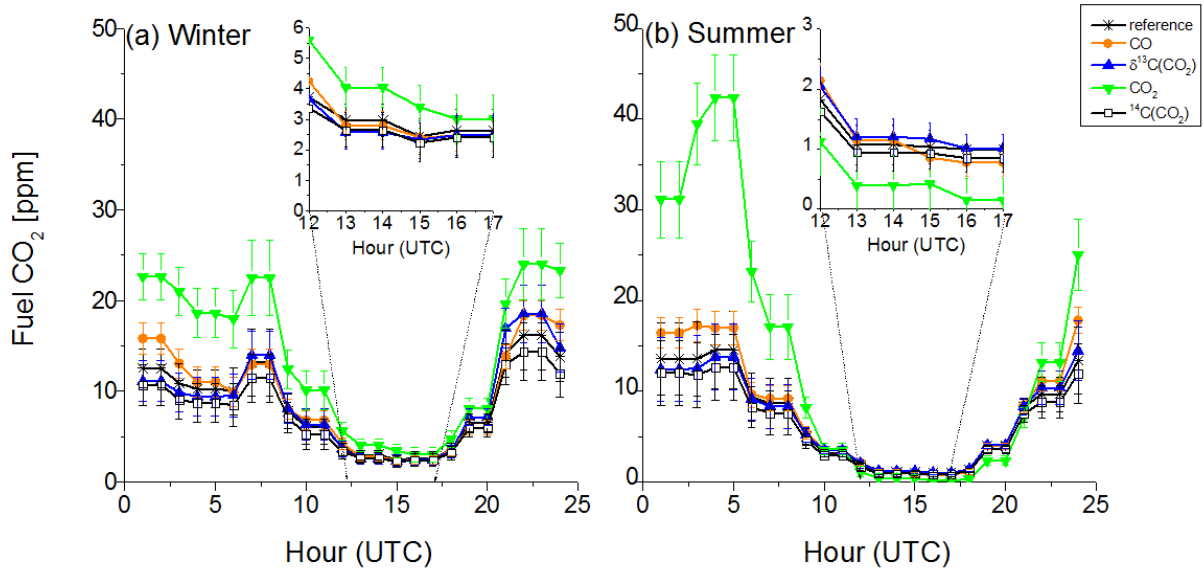


1

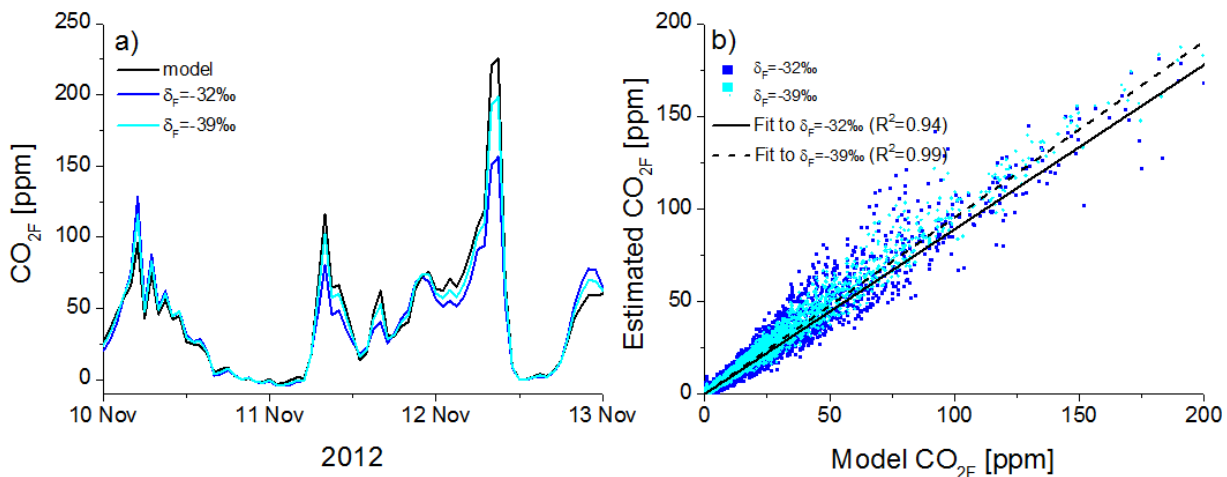
Difference fuel CO₂ [ppm]: model - estimated

2 Figure 7: Same as Fig. 3, but now also including measurement imprecision.

3



1
 2 Figure 8: Comparison of median diurnal cycle of fuel CO₂ given in model reference or estimated
 3 with one of six different tracer methods at the measurement station Heidelberg. Error bars denote
 4 the standard error of the fuel CO₂ estimate at each hour for the respective half year. The diurnal
 5 cycle of the CO + $\delta^{13}\text{C}(\text{CO}_2)$ methods are not shown, since they are very similar to the $\delta^{13}\text{C}(\text{CO}_2)$
 6 method.



1 Figure A1: a) Example period showing fuel CO₂ of different fuel CO₂ estimation methods and
2 reference modelled fuel CO₂. Dark blue: Mean δ_F is -32 ‰, cyan: mean δ_F is -39 ‰. b) Correlation
3 plot between estimated and modelled fuel CO₂ for mean $\delta_F = -32$ ‰ (dark blue and solid line) and
4 mean $\delta_F = -39$ ‰ (cyan and dotted line) during entire year 2012. Fuel CO₂ can be estimated much
5 better using $\delta^{13}\text{C}(\text{CO}_2)$ when the fuel $\delta^{13}\text{C}$ signature is strongly depleted with respect to the
6 biosphere. Note, that the slope slightly changes when using more depleted sources. This is because
7 few high fuel CO₂ peaks span the linear regression and therefore determine the slope to a large
8 degree, but as a general tendency for the Heidelberg data set the high fuel CO₂ peaks exhibit an
9 isotopic signature, which is more enriched as the isotopic signature of the mean fuel source mix.